A System for Optimizing Interior Daylight Distribution Using Reflective Venetian Blinds with Independent Blind Angle Control

by
Molly E. McGuire
B.S. Mechanical Engineering 1999, Stanford University

Submitted to the Building Technology Program in the Department of Architecture in partial fulfillment of the requirements for the degree of

Master of Science in Building Technology

at the

MASSACHUSETTS INSTITUTE OF TECHNOLOGY

June 2005

Signature of author:_____
Building Technology Program
Department of Architecture
May 6, 2005

Certified by:_____
Leon R. Glicksman
Professor of Building Technology and Mechanical Engineering
Thesis Advisor

Certified by:_____
Marilyne Andersen
Assistant Professor of Building Technology
Thesis Advisor

Accepted by:_____
Adèle Naudé Santos
Acting Head, Department of Architecture
Dean, School of Architecture and Planning
Chairman, Committee on Graduate Students

A System for Optimizing Interior Daylight Distribution Using Reflective Venetian Blinds with Independent Blind Angle Control

By

Molly E. McGuire

Submitted to the Building Technology Program in the Department of Architecture on May 6, 2005 in partial fulfillment of the requirements for the degree of Master of Science in Building Technology

ABSTRACT

An operational algorithm for blind angle control is developed to optimize the daylighting performance of a system of reflective Venetian blinds. Numerical modeling and experiment confirm that independent control of alternating blinds yields adequate visual comfort and daylight distribution to a distance of 10 m from the window under most clear sunny and overcast sky types. Under overcast sky conditions, all blinds are set to a uniform angle which optimizes light redirection to 10 m. For cases of direct solar incidence, alternating blinds are used for shading and light redirection and adjusted with changing solar position. For low solar angles, a set of blind angle configurations is developed utilizing blind-blind reflections to maximize light penetration.

Thesis Supervisor: Leon R. Glicksman
Title: Professor of Building Technology and Mechanical Engineering

Thesis Supervisor: Marilyne Andersen
Title: Assistant Professor of Building Technology

Acknowledgements

I would like to thank everyone who has helped me create this work over the past two years. I would like give special acknowledgement to

Leon Glicksman, for his intellectual guidance and commitment to the end,

Marilyne Andersen, for her support and academic rigor,

Jean-Louis Scartezzini, Pierre Loesch, Anothai Thanachareonkit and the many others at EPFL who generously gave of their time, intellect, and kindness during my stay,

Kathleen Ross and Nancy Dalrymple, for their kindness,

The many others at MIT and other institutions who freely gave of their time and advice,

The Cambridge Science Foundation of America, for enabling my research at EPFL through a generous grant,

The Institute, for enabling independent exploration and research through a Presidential Fellowship

My father, for reading this thesis cover to cover,

Julien, for putting aside his own work so many times to serve as my sounding board, and for his emotional support,

My friends and family, for keeping me smiling, and

My parents, for their love, their confidence in me, and their support without which I would not be here.

Building Technology Laboratory
Massachusetts Institute of Technology

1 Introduction

1.1 Background

As world population grows and, with it, the consumption of a shrinking supply of finite resources, it is necessary to rethink consumption patterns in an attempt to create a more sustainable society. The United States alone consumes 26% of the world's annual budget with only 5% of the population; Europeans consume less per capita, but still far more than most countries. (1) In the U.S., buildings consume roughly one third of the total energy and two thirds of total electricity. Building lighting needs account for 37% of the total electricity consumption. (2)(3) Improvements in the last 25 years have increased lighting efficiency, resulting in an marked decrease in energy consumption, yet there is still opportunity for significant reduction in total annual energy consumption by minimizing electric lighting requirements. Building designers can impact overall energy demand by pursuing in parallel the complementary goals of reduction in demand and increase in efficiency. Demand reduction includes, among other things, making maximum use of available natural light.

Additionally, many studies have shown that naturally lit buildings provide significant benefits to occupants when compared with electrically lit buildings. A 1999 study showed that test scores of students in schools mainly lit by daylight showed a 26% increase over those of comparable students in classrooms with only electric light, and a 10% increase compared with students in average classrooms. (4) Two years later, the same study was undertaken by the New Building Institute as a peer review and the results were confirmed. (5) Advanced daylighting design helped drive a 16% increase in worker productivity at Lockheed's Building 157 in California, and similar increases in case studies across the country. (6)

During the energy crisis of the 1970's, concerned building designers advocated daylighting as a path to consumption reduction. The sun provides sufficient natural light to meet office workspace lighting conditions, even on a cloudy days. Although investigation of daylighting techniques has been ongoing for more than 30 years, the optimism of the 1970s has not lead to high market penetration today. Explanations range from lack of effective modeling tools to the prohibitive cost of equipment and construction. In addition, the most efficient daylighting technologies reduce electricity consumption only to the extent that they are coupled with systems that dim electric lights. A workable daylighting solution is cost effective, practical, versatile, and flexible, lending itself to application in a large percentage of commercial building projects.

1.2 Literature Review

The oldest and most common form of daylighting, the untreated window or opening, is still a popular and relatively inexpensive method for introducing natural light into the interior space. However, direct window lighting has limited benefit and potential negative effects. Lighting levels from the untreated window decrease asymptotically with distance from the window, and typically can reduce electric lighting needs only within a 15-foot distance from the window. Skylights can introduce natural light throughout the floor plan, but may allow unwanted direct sun transmission when the sun is highest in the sky. For some applications and with proper controls, these daylighting solutions are appropriate. Smaller buildings with a high surface-area-to-volume ratio can meet a large percentage of lighting needs through windows and skylights. However, often the proposed daylighting solution maximizes the glazed portion of the façade, resulting in increased cooling loads and overheating due to direct sun, and unpleasant lighting conditions for occupants near the window. (7)

Large-scale buildings attempting to incorporate sustainable building technologies often make use of more customized daylighting solutions and often use atria and other open spaces to introduce natural light. The Genzyme Building in Cambridge, MA, for example, utilizes sun-tracking heliostats to redirect sunlight downward into an open central atrium, where the light is diffused by a complex prismatic chandelier. Diffuse light from the atrium is then brought into office spaces in the surrounding floors by

special reflective vertical panels. In addition, Venetian blinds with a semi-specular finish direct daylight from the outside in through the façade. (8)

Under typical commercial building design conditions, however, designers must deal with more stringent space and budgetary constraints when meeting lighting and occupant comfort needs. Most commercially available daylighting systems address these requirements by providing one of two functions: shading or light redirection. Shading devices, such as prismatic panels, the brise-soleil, exterior lamella, and Venetian blinds, address the issues of excessive solar gain and occupant visual comfort. More recently developed advanced glazing materials with variable or selective transmission properties. (9) Both serve to reduce or prevent direct solar incidence, while still gaining some benefit from daylighting. Often, though, attempts to prevent unwanted direct sun result in insufficient light provided to occupants' workspaces. This shortfall is made up for with electric lighting. In the worst cases, the light is blocked by internal shading devices, such as an internal Venetian blinds system in the closed position, is absorbed by the blinds, and results in an additional cooling load without providing any daylighting benefit.

To increase benefit from daylighting in buildings, designers have developed active and passive technologies to redirect light into the interior of the building while minimizing the negative effects of direct sunlight into the space. Such strategies include reflective architectural elements such as the light shelf, light tube, laser-cut panel, fiber optics system, sometimes coupled with a sunlight concentration system, and others. While these elements may effectively increase light to the interior, they are not practical lighting solutions for most buildings. Most require specialized design expertise, are highly customized, and often consume valuable interior volume. In addition, slight design modifications during construction or a post-construction retrofit may render these elements ineffective. For example, a naturally-ventilated building, Houghton Hall in Luton, U.K., was designed with interior light shelves as part of an energy-saving design. Below the light shelves, the glazing was left untreated. Occupants complained about glare resulting from the uncovered window area below the light shelf and as a result Venetian blinds were installed, covering the entire window, including the light shelf, and rendering the redirection device ineffective. (10)

While many active systems are prohibitively expensive, most passive technologies, including the light shelf system, lack the flexibility to create acceptable interior lighting conditions under changing outdoor sunlight conditions. The reflection angle of the shelf and light inlet aperture are fixed to optimize interior lighting at certain times of the day and year. The reflectance geometry of a light-redirecting element depends on incidence angle (dictated by time of day and year, façade orientation) and specular and diffuse components of the light source. Fixed-angle light shelves can be optimized for a specified set of conditions, but may be far less effective under other lighting conditions. Additionally, the area through which light enters the façade must be designed for a particular sky condition; the window size required to allow sufficient lighting on an overcast winter day may create excessive solar gains on a clear sunny day. Allowing more light to enter the building than is dictated by lighting requirements results in unnecessary additional cooling load.

A number of physical characteristics also contribute to the unsuitability of light shelves as a daylighting solution for most situations. The internal space required for an effective reflection surface area is often intrusive and architecturally unfavorable. Beltràn et al studied a light shelf system with a 1.4-meter horizontal shelf located at a height of 2.4 meters above the floor. While sufficient to achieve an illuminance level of over 200 lux year-round at a distance of 8.4 meters from the window, the size of this element is not architecturally practical. In order to minimize intrusion into the room, they also studied multi-level systems which achieved similar illuminance levels utilizing smaller shelves, more reflective area, and a larger window aperture. (11) Their finding suggest that increasing that increasing the number of shelves or reflectors while decreasing the width might be a preferable solution.

Another light redirection technology, the light pipe system, can be used to transport light far into the interior of a building and delivered to workspaces through openings in the ceiling or walls. Beltràn et al. found that light pipes have the advantage of giving the designer a high level of control over geometric distribution of light within the space, relative to light shelves. While this technology allows sufficient lighting to penetrate far into the building without creating unacceptable levels of lighting at the perimeter, the

practical limitations suggest that this technology is not appropriate for widespread implementation. The light pipe transport system requires a transport shaft running from the collection source (rooftop, outside wall, or other) to the distribution point(s) within the building. This pipe often consumes valuable volume within the ceiling plenum. In addition, the multiple reflections required to transport and diffuse the light beam result in diminished intensity, which may or may not be problematic, depending on outdoor lighting conditions. (11)

Fiber-optic systems are more flexible and less intrusive than light pipes, but require a similar level of custom design. The system necessarily requires a solar collection/concentration system because of the relatively small diameter of the transport medium. This component, often active tracking the sun, in addition to the custom equipment and design required for the system, makes light transport via fiber a costly option not appropriate for widespread application.

These specialized systems have a place in specific architectural applications—high-end projects or small-scale buildings or houses—but have not proven to be practical for most commercial building stock. Custom design elements translate directly into additional cost and potential for delays in construction. A daylighting-redirection system integrated into a standard fenestration system could potentially lead to more widespread usage.

Venetian Blinds

The Venetian blind fenestration system has been widely studied as a shading system, and less frequently as a light-redirecting system. Venetian blind manufacturers currently offer many reflective Venetian blind options. European companies such as Warema, Hüppe, and Retrosolar offer automated reflective blinds designed to provide adequate shading and to increase light levels. In these systems, all blinds are controlled as a group, without flexibility for individual blind control. In some cases, the blinds are split into two groups, with the upper half of the blinds optimized for light redirection and the lower half angled to prevent uncomfortable lighting conditions at the workplane.

To date, research in Venetian blinds has focused on changes in interior lighting levels and cooling loads due to a change in geometry, occupant control, blind angle (static and

automated), and other similar areas. The International Energy Agency (IES) commissioned tests on the effect on indoor lighting conditions due to various types of Venetian blinds, under overcast and sunny conditions. Blind types included: standard light gray coated, semi-specular, static vs. automated, translucent, semi-silvered, semi-silvered translucent (manufactured by Hüppe), and the "fish" system (fixed horizontal louvers with a triangular cross-section). Results showed a decrease in illumination level throughout the room, as compared with a reference room with uncovered window, for all blind types except the "fish" system, which outperformed the reference room at high solar altitudes at certain times of the year. The authors concluded that none of the tested systems markedly increased lighting levels at distances of 6 - 8 m from the window as compared with the uncovered window. (9)

Lee et al demonstrated that an automated Venetian blind system yielded significant energy savings (in both lighting and cooling load) and peak demand reduction as compared to a similar system with a static blind angle. (12) Their research focused on optimizing the energy balance between electric lighting and thermal gain, as affected by daylight brought into the building by semi-specular Venetian blinds within a two-pane tinted glazing system. Blind slat angle was actively adjusted in response to a control system monitoring a photosensor on the test room ceiling and sensors monitoring cooling loads. Blind angle was adjusted every 30 seconds to block sun while maintaining an illuminance of 540 to 700 lux at 2 – 3 m from the window (a 1:1 or 1:2 distance to window height ratio, for a window height of approximately 2 m above the workplane), if possible under current outdoor lighting conditions. Although measured workplane illuminance levels for the experiments are not given, the results do show significant savings in both cooling load and lighting energy and suggest that a finer control of blind angle (i.e. control of individual blind angle) would further increase energy savings.

In the late 1970's, Rosenfeld et al investigated a fenestration system incorporating multiple types of blinds along the height of the window. (13) The proposed system included silvered "beam blinds" at the top of the window and more traditional diffuse blinds for shading lower part of the window. The system was designed to reflect sunlight deep into the room (up to 30 feet) and shade the area close to the window. They

hypothesized that seasonal adjustments and uniform blind angle would be sufficient under all lighting conditions and calculated a 2 to 3.2 year payback for capital investment.

More recently, Breitenbach et al developed a model to sufficiently predict the lighting and thermal effects as a function of blind angle and geometry for a double glazing system with integral Venetian blinds at a uniform blind angle. (14) Blind material was metallic but non-mirrored (90% diffuse). This model can be used to study the effects of small changes in blind design and operation for this type of blinds. Among other findings, they discovered that, in the case where blind angle is adjusted so that all light entering the test room is transmitted by multiple reflections, blind geometry strongly influences spatial distribution of light. Combining both the thermal and optical transmission of a particular uniform blind configuration, this model may be useful in determining the balance point between energy saved from reduced lighting needs and energy consumed from additional cooling load.

Another study of integrated Venetian blind performance by Tzempelikos and Athientis focused on maximization of daylight transmission and view to the outside without allowing direct sunlight penetration. Tested blinds were "highly reflective," although specular/diffuse components were not given. Blinds were tested at uniform slat angle, and results show that the blind configuration allowing the greatest combination of daylight transmission and view for overcast conditions is the horizontal position. Under sunny conditions, all blinds must be set to the minimum angle necessary to block direct transmission, facing outward toward the directing of the incident rays. The study investigated visible and solar transmittance through the blinds, but did not measure workplane illuminances and penetration depth of transmitted light. (15)

1.3 Research Goals

The typical commercial office building daylighting system aims to achieve visual comfort by addressing four lighting parameters:

1) Direct sunlight The prevention of direct sunlight transmission onto the workplane is a primary concern in system design. Direct sun can cause thermal discomfort from overheating, high contrast ratios, and glare on computer monitors and other specular surfaces. Except in select circumstances (lighting accents or other aesthetic effects), direct sunlight transmission is to be avoided.

2) Illuminance level The recommended horizontal workplane illuminance level given by the Illumination Engineering Society of North America (IESNA) for normal desk work is 300 - 500 lux, depending on intensity of computer usage. (16) The Institute for Research in Construction, part of the National Research Council Canada, recommends 400 – 500 lux for open-plan office space (18) and the Commission Internationale de l'Eclairage (CIE) recommends a minimum of 400 lux. (19) The current study aims to achieve workplane illuminance levels of 400 lux, with the understanding that values not less than 300 lux may be acceptable in some circumstances.

   Daylight factor, or ratio of illuminance at the workplane to the global horizontal illuminance outside, is often used to quantify a daylighting system's response to overcast sky conditions, as an alternative to absolute illuminance values. CIE recommends a minimum daylight factor for office work of 2%.

3) Light penetration A typical "rule-of-thumb" standard for lighting designers predicts that a window will provide sufficient illumination up to a distance one and a half to two times the height of the window. (20) In other words, a 2 m-high window should be able to provide sufficient light to 3 to 4 m. This window height refers only to window area above the level of the workplane; light entering the window below desk height will likely be absorbed by furniture and floor. For this study, a daylighting system that effectively increases light penetration will be defined as one that increases

this ratio, with the goal being sufficient daylighting at a distance of 10 m, or a 1:5 height/depth ratio for a 2 m window.

4) Luminance ratio and glare A moderately high contrast can cause visual discomfort and a high level can cause glare and even momentary blindness. Discomfort can be avoided by limiting the contrast ratio to 1:3 between task and adjacent surroundings, and 1:10 between task and remote non-adjacent surfaces. (16) One source of high contrast conditions is glare from flat surfaces such as desktops or computer monitors. Nearly all glare can be avoided by eliminating direct sun transmission in office space programmed for desk work.

5) Illuminance distribution In order to avoid high contrast ratios between surfaces close to and far from the façade which can create the perception of low lighting levels even when there is sufficient light, it is necessary to moderate the light distribution throughout the space. The maximum variation in field-of-view luminance should not exceed a ratio of 1:10, and therefore surface illuminance variations are limited to the same ratio.

Additionally, qualitative characteristics of an ideal daylighting system include: simplicity (to minimize cost), elegance as an architectural element, and the ability to provide occupants with a view to the outside.

As shown in the preceding sections, a variety of technologies have been proposed to address these issues. One set of technologies (including light shelves and roof-top fiber optics) uses active means to redirect sunlight in order to increase illuminance levels, while another set (shading devices and Venetian blinds, for example) primarily addresses the need to block direct sunlight transmission. The aim of this thesis is to investigate the optimal operating conditions for a system that integrates these goals—mirrored reflective Venetian blinds. These blinds are used to redirect both direct and diffuse light to the ceiling, which in turn reflects the light to illuminate the workplane. Ideally, this system optimizes interior lighting conditions (thereby minimizing dependence on electric lighting) for both overcast and clear sunny days while maximizing visual comfort.

To be effective, the blinds must achieve these goals over a range of possible sky conditions. For clear sky conditions, the blinds must respond to changing sun altitude and azimuth, directing discrete beams of light to the ceiling. For overcast skies, the blinds must optimize redirection of the diffuse sky light from the entire sky dome. Two models have been developed to handle these general sky types. In order to explore the full potential of reflective Venetian blinds to address these design conditions, each blind slat is allowed to move independently of the rest. Although it would be quite cumbersome to implement a system with individual controls for each blind, this was the theoretical starting point for investigation.

It will be shown that these requirements can be met for nearly all sky conditions through a reflective Venetian blinds system that utilizes control of two separate blind groupings: the even-numbered and the odd-numbered blinds. This is accomplished for clear sky/direct sun conditions by tuning one grouping of blind slats to the optimal position for redirecting light far into the space, and the other to the correct position to achieve sufficient shading to prevent direct sun on the workplane. Under overcast sky conditions, optimal lighting can be achieved by setting all blinds to a single optimized blind angle. The evidence supporting these conclusions, and the range of tested solutions is presented in the following chapters. Chapter 2 of this thesis discusses modeling and optimization techniques and test results for overcast sky conditions and Chapter 3 discusses the same for clear sky/direct sun conditions. Chapter 4 concludes by suggesting a preliminary design for the blinds and areas for further exploration.

2 Blind System Performance: Overcast Sky Conditions

2.1 System Design for Numerical Modeling

In order for a façade-based daylighting system to improve the lighting conditions within a space relative to an uncovered window, the system must redirect daylight from the front of the room (close to the window) to the rear of the room. A successful daylight redirection system will increase the workplane illuminance levels at distances of 5 to 10 meters from the window for both sunny and overcast skies, while managing the other aspects of visual comfort. Reflective blinds accomplish this by redirecting daylight to a highly reflective ceiling, which then redistributes the light to the workplane.

The amount of light incident on the workplane for a given window opening is a function of many variables including incident light on the ceiling, reflection coefficients of ceiling, walls, and furniture, and directly transmitted light (light that is not reflected or absorbed by the blinds). In order to isolate the dependence of light distribution on blind configuration, it is necessary to isolate relevant variables. Therefore, for initial modeling purposes, only the light redirected by the blinds and incident on the ceiling will be considered, and this will function as a predictor of light received by the workplane. The model neglects light reflected by the walls or floor to the ceiling. The implicit assumption is that an increase in light received by the ceiling will result in an increase in incident light on the workplane. This assumption is later confirmed by experimental workplane illuminance results for overcast sky conditions and used to predict workplane illuminance modeling for direct sun conditions. The reflection on surfaces within the space is neglected in them model for simplification purposes and the model does not take into account diffuse light transmitted directly through the blinds directly to the workplane (confirmed to be relatively small through physical simulation, as demonstrated in Section 2.5).

The response of the blinds system is modeled in Microsoft Excel. The room is modeled 2-dimensionally as a rectangular space with a height of 3 m and a depth of 10 m. The glazed portion of the space is 2 m high, extending from a height of 1 m to the ceiling (3 m). The blinds cover the entire glazed segment. The 20 Venetian-style (horizontal) blinds are 10 cm wide, flat, of negligible thickness, and uniformly spaced 10 cm apart. Each blind angle may be adjusted independently. The workplane is assumed to be at a height of 1 m from the floor. The blinds have a purely specular reflective upper surface, and a purely black lower surface.

Sections 2.2 and 3.1 discuss modeling under overcast and direct sun conditions, respectively.

2.2 Numerical Modeling for Overcast Sky Conditions

In order to model the ceiling illumination due to the reflection of an overcast sky onto the ceiling by the blinds, it is necessary to determine the portion of the sky "seen" in the reflection on each blind at every point on the ceiling. From a given point on the ceiling, the eye will see a portion of sky in the reflection on the blind, as if seeing directly through the blind to a virtual image of that sky portion. Figure 2.2.1 shows the virtual image seen from an arbitrarily chosen point on the ceiling through a horizontal blind. This virtual image will be used, in part, to determine the light reflected by the sky to each point on the ceiling.

To model the sky luminance seen by each point along the ceiling, the ceiling is conceptually divided into segments 0.25 m in length, and the reflected light to each segment is calculated separately. The illumination received by each segment is modeled by calculating the configuration factor between each ceiling segment and the virtual image of sky (as reflected about the reflection plane of the blind). For each blind, the sky is modeled as a 2-dimensional isotropic white Lambertian diffuse horizontal plane, extending 10 m outward, which can be considered infinite relative to the scale of an individual blind, from the edge of the blind immediately above. The system is assumed to be infinite in the z-direction (i.e., the direction of the length of the blinds). For each blind, the model reflects this horizontal sky plane about the plane of reflection of the blind, and then calculates the configuration factor between this reflected surface and a given ceiling

segment, which represents the portion of this reflection "seen" by the ceiling through the reflective surface of the blind. A schematic showing the horizontal sky plane reflection about one blind is shown in Figure 2.2.3. This model also takes into account any masking effects of the blind immediately above.

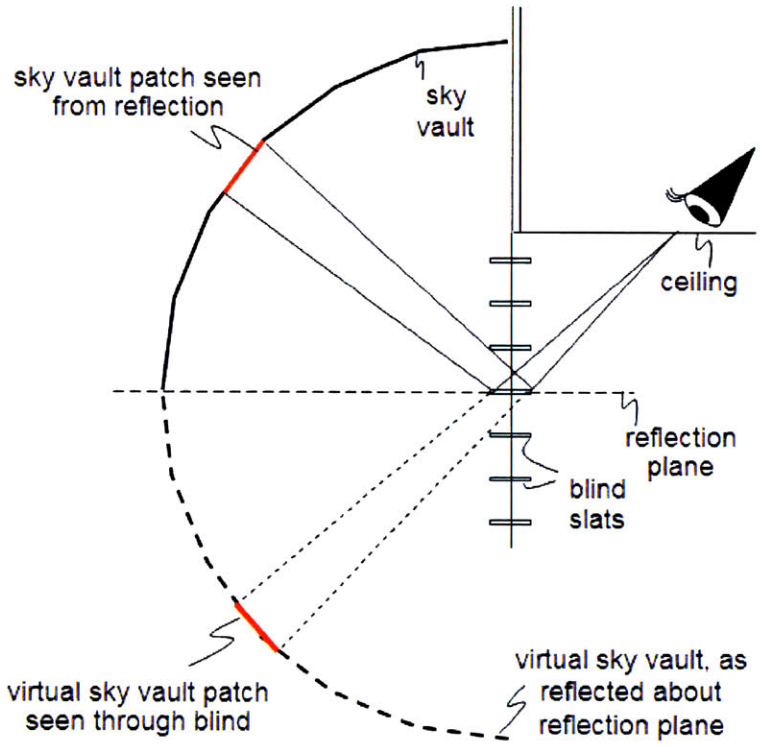

Figure 2.2.1 Real and virtual sky views seen by a point on the ceiling through a reflection on a mirrored blind

The model calculates the flux contribution from the sky, reflected by each blind, to each ceiling segment and then sums the 20 contributions, dividing by the area of the segment, to calculate incident illuminance on each ceiling segment. The exitance of the sky plane is converted into flux and corrected for the reflectivity of the blind, as shown in the following equation,

$$E_C = \frac{\rho F_{S-C} M_S A_S}{A_C} \qquad (2.2.1)$$

where E_C is the luminous illuminance on the ceiling segment [lux], ρ is the reflection coefficient of the blind, $F_{R\text{-}C}$ is the reflection-to-ceiling configuration factor, M_S is the luminous exitance from the sky plane [lux], and A_p and A_c are the areas of the sky plane and ceiling segments, respectively [m^2].

The absolute value of the chosen sky plane exitance is not important, as the model calculates daylight factor, which is a ratio of measured diffuse interior illuminance to measured exterior global horizontal illuminance. The daylight factor, measured for buildings only under overcast sky conditions, takes into account the three contributors to interior lighting: direct light (from the part of the overcast sky dome "seen" by the point of measurement), reflected exterior light, and reflected interior light. As the model assumes all exterior and interior reflection coefficients to be negligible, the single contributor to interior illuminance will be direct sky light reflected to the ceiling by the reflective blinds. Hereafter, this measured ratio at the ceiling is referred to as illuminance ratio, because the term "daylight factor" refers specifically to illuminance measured at the workplane, not at the ceiling. The exterior global horizontal illuminance is taken to be equivalent to the exitance of the sky plane.

Modeling the sky as a Lambertian 2-dimensional horizontal plane introduces some limitations. First, effects of the 3-dimensional nature of the real sky will not be captured because incident light from any azimuth angle other than 0°, or normal to the blinds, is not taken into account. Second, this sky model closely simulates an isotropic overcast sky. However, the assumption that the plane emits uniformly does not take into account other overcast sky types (for example, a CIE standard overcast sky with a luminance ratio of 3:1 between the zenith and the horizon). For the purpose of this investigation, only isotropic overcast skies will be considered.

Configuration Factor

The configuration factor between the reflection and the ceiling is calculated using a method commonly used to calculate radiant heat transfer between two surfaces. In heat transfer, the configuration factor can be used to quantify the ratio of flux (W, for

example) emitted by one surface to the flux received by another surface. Light exchange, also electromagnetic radiation, can be treated in the same manner. In photometric terms, the configuration factor is the ratio of flux (lumens) emitted from one surface to the flux received by another surface. In radiometric terms, flux received by surface B, q_B, can be calculated,

$$q_B = F_{A-B} q_A \qquad (2.2.2)$$

where q_A is the flux emitted by surface A and F_{A-B} is the configuration factor from surface A to surface B. For photometric quantities, a relationship between luminous exitance (lm/m^2) emitted from and surface and illuminance (lm/m^2) received by a surface can be formed using the configuration factor between the two surfaces. In this case, the areas of the emitting and receiving surfaces, A_1 and A_2 respectively, are used to calculate the total flux emitted or received by the surfaces. Equation (2.2.3) shows the relationship between illuminance received by surface 2, E_2, and exitance emitted by surface A_1, M_1,

$$E_2 = \frac{F_{1-2} M_1 A_1}{A_2} \qquad (2.2.3)$$

The crossed-strings method, first discovered by Hottel, is used to determine the configuration factor for radiant heat transfer between two Lambertian surfaces within a long enclosure that has a constant cross-section (i.e., a system that can be approximated as 2-dimensional). (21) This method may also be used for photometric transfer, granted that the surfaces diffuse visible light according to a Lambertian distribution. In the crossed-strings method, four strings (shown in red) are attached to the edges of the two surfaces in question, two crossed and two uncrossed as shown in Figure 2.2.2. The strings are then pulled taught around any obstructions.

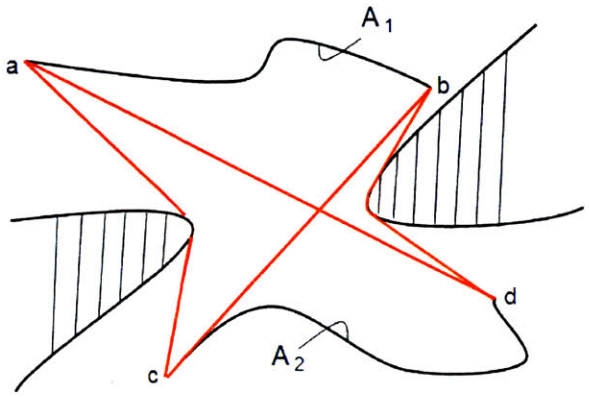

Figure 2.2.2 Example of crossed strings method between surfaces A1 and A2

The lengths of the four strings (distances ad, bc, ac, and bd) are used in the following calculation to calculate the configuration factor of surface A_1 on surface A_2,

$$F_{1-2} = \frac{(A_{bc} + A_{ad}) - (A_{ac} + A_{bd})}{2A_1} \qquad (2.2.4)$$

In the case of the blinds system, each reflective blind is treated as a mirror through which the ceiling can "see" a reflection of the sky. For each blind, the sky is modeled as an isotropic plane extending horizontally from the blind immediately above. This sky plane is reflected about the axis of the blind. The configuration factor between this reflection and each ceiling segment is then calculated. In calculating configuration factor using the crossed strings method, the strings attach at each edge of the sky reflection, pass through the reflective surface of the blind, and attach again at each edge of the ceiling segment. The edges of the blinds serve as the corners around which the strings are pulled tight. Figure 2.2.3 shows the strings attached at the edges of the sky plane reflection and at the edges of the ceiling segment. Depending on blind angle, the blind immediately above can

serve to reduce the configuration factor by partially blocking the path between reflection and ceiling segment, as shown in Figure 2.2.3.

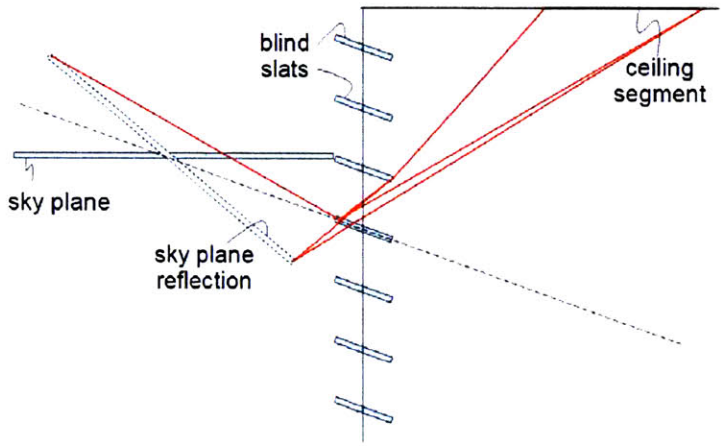

Figure 2.2.3 Crossed strings geometry for a reflective blinds system

Optimization

Under overcast sky conditions, there is no risk of direct solar transmission through the blinds. Therefore, the driving parameter for optimization of the blinds system is illumination level at the back of the room. An additional parameter for consideration during the optimization is ratio of maximum to minimum illuminance level across the ceiling. The optimization was performed using Microsoft Excel's Solver function, which adjusted each blind angle to find a maximum illuminance value on the 9.75 – 10 m ceiling segment.

Figure 2.2.4 show the illuminance ratio distribution, as a function of distance from the widow, for the case in which each blind is set to the horizontal position. The peak ceiling illuminance ratio of 16% occurs close to the window, at an approximate distance of 1 m. Levels decrease to ¼ of this value at 3 m. Beyond 6.5 m, values are below 0.5%. As noted previously, this illuminance ratio at the ceiling is not equivalent to expected workplane illuminance levels, and therefore can not be compared with recommended

daylight factor values, but will serve as a metric to make relative comparisons between potential optimized solutions.

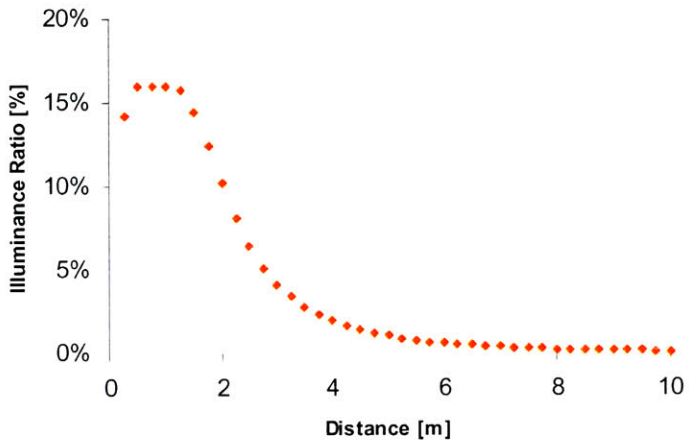

Figure 2.2.4 Illuminance ratio as a function of distance from the window for a horizontal blind configuration, ρ = 95%, blind spacing is equal to blind width

Optimal blind angles range from 19° for the bottom blind to 26° for the top blind, where a positive blind angle signifies a tilt of the top surface in toward the interior. In order to test the increase in back-of-the-room illuminance level gained by allowing each blind to be positioned at a unique angle, this scenario is compared with two other scenarios in which the blinds are grouped into four segments (5 blinds per segment) and one segment (20 blinds per segment) and the blind angle is optimized for each segment as a whole. For the 4-segment scenario, the model gives the optimal angles for the four segments starting from the top segment: 24°, 23°, 21°, and 20°. For the single segment case when all 20 blinds are set to the same angle, the model yields an optimal angle of 21°. Figure 2.2.5 gives a comparison of the three scenarios. The change in illumination at the back of the room is significant compared with the horizontal blinds configuration (greater than a factor of 3), but is negligible among the three cases. This would suggest that illuminance level at the back of the room is not strongly dependent on the flexibility to set the blinds to distinct angles.

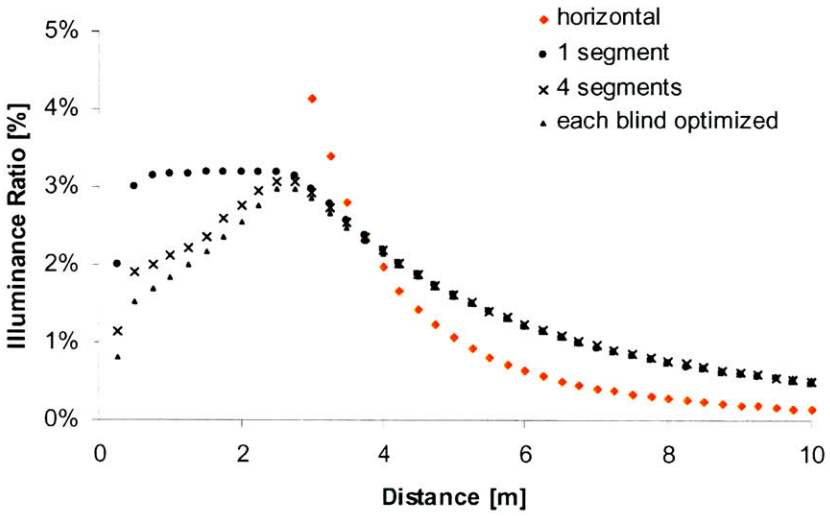

Figure 2.2.5 Illuminance ratio as a function of distance for three optimized scenarios, compared with horizontal scenario

A comparison of the light contribution of each blind to total illuminance at the back of the room explains this observation, as shown in Appendix A for each of the three scenarios. In each case, the bottom blind contributes more by a ratio of roughly 15:1. Therefore, it is not surprising that the optimal angle, 21°, for the single segment case (in which all 20 blinds are set to the same angle) is fairly close to the optimal angle for the bottom blind alone, 19°, and quite a bit less than the optimal angle for the top blind alone, 26°.

2.3 Scale Modeling for Artificial Sky Simulation

Physical testing of the blinds systems was carried out both to test the accuracy and optimization techniques of the numerical models in predicting light reflected to the ceiling, and to test the resulting workplane illuminance due to ceiling illumination. Experiments were carried out under artificial sun and sky simulators were performed with the assistance of the Solar Energy and Building Physics Laboratory (LESO-PB) at

L'Ecole Polytechnique Federale de Lausanne, Switzerland (EPFL). Daylight experimental facilities at LESO-PB include a goniophotometer, used to test the bi-directional transmission (reflection) distribution function, or BT(R)DF, under direct solar conditions, and a heliodon/scanning sky simulator, for simulating the diffuse sky component. (22)(23)

Modeling

The model used for testing at LESO-PB was constructed at a 1:10 scale, shown in Figure 2.3.1. The reflective blinds are fabricated from 1/32-inch coated aluminum lighting sheet, cut to dimensions of 1 cm by 24.6 cm on a jump shear. In order to stiffen and straighten the aluminum, two pieces are laminated together, back to back, with epoxy. The 0.1-cm thickness of the two laminated sheets is calculated to be within an acceptable range so as not to cause significant interference effects due to blind thickness (i.e., the blinds can be assumed to have negligible thickness). One side of each of the blinds was painted black. Twenty identical blinds were placed in a milled aluminum frame, spaced 1 cm apart and held by milled brass pins. Figure 2.3.2 shows a photograph of the assembled frame and blinds, attached to the model.

The blind positions are set manually, using a custom-built angle adjuster, fabricated out of clear acrylic on a laser cutting machine. The angle adjuster, shown in Figure 2.3.3, attaches directly to the edge of the blind, and then adjusts the angle of the blind relative to etched lines on a piece of black acrylic that attaches perpendicularly to the blinds. The brass pins are held in place with set screws (not shown in drawing, but seen on the left side of the frame in Figure 2.3.2), securing the blind in the measured angle position. The blind angle adjustment mechanism allowed 0.5° angle adjustments, however the system was determined to be accurate to within ±2°.

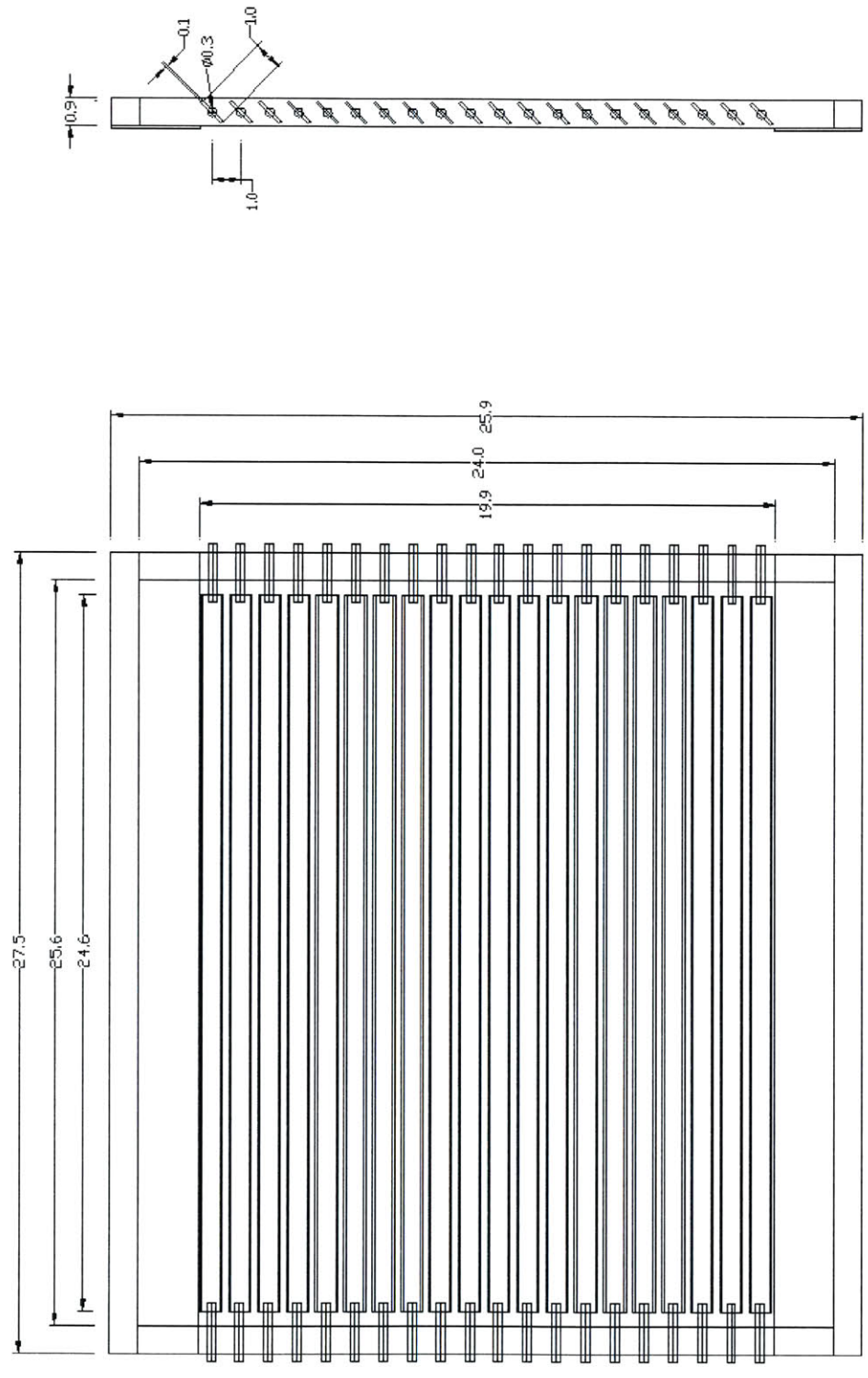

Figure 2.3.1 Scale drawing of blinds and frame, dimensions in cm

Figure 2.3.2 1:10 scale model of reflective blinds, attached to model for overcast sky simulations

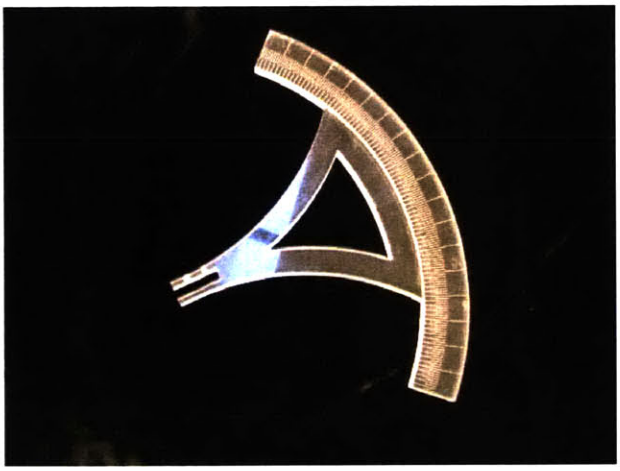

Figure 2.3.3 Blind angle adjuster attaches directly to blind and rotates relative to fixed etched lines

An artificial sky dome was used to simulate the diffuse component of the sky. Unlike the goniophotometer which tests the transmission function of a single fenestration sample, the sky dome is used to test the response of a complete architectural model to varying sky conditions. The sky dome consists of 25 luminous discs which comprise a sixth of a hemisphere. An architectural model of interest, in this case, a test room with blinds covering an opening at one end, is mounted on the heliodon, which can be rotated about two axes to simulate any building orientation. Figure 2.3.4 shows a schematic, in plan

view, of the sky simulator, heliodon, and model and Figure 2.3.5 shows a photograph of the test setup.

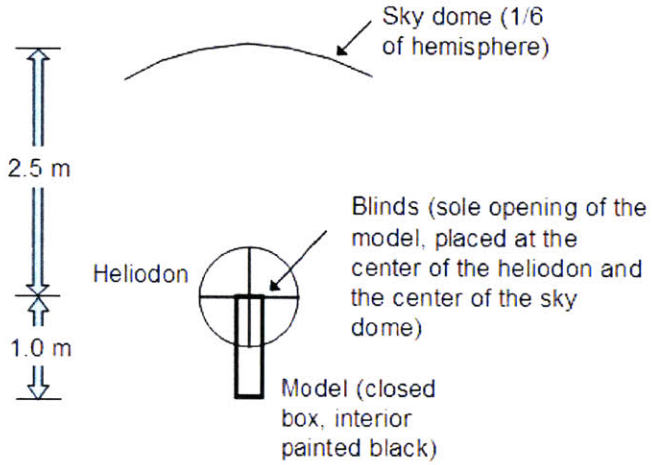

Figure 2.3.4 Plan view of scanning sky simulator, showing sky dome, heliodon, and model orientation

Figure 2.3.5 Scanning sky simulator, heliodon, and model

Small-scale photosensors (LMT Pocketlux-2, 1-cm sensing area) are positioned within the model at points of interest. One photosensor is positioned below the sky dome, unobstructed, in order to measure the global horizontal illuminance necessary for calculation of daylight factor. In order to perform a test with the entire hemispherical sky dome, the heliodon is then rotated six times and successive illuminance measurements

are taken at every 60° interval. The six illuminance measurements taken by each photosensor are summed, and divided by the sum of the global horizontal illuminance readings for each of the six heliodon positions to yield the daylight factor for that particular interior photosensor position. In order to measure interior illuminances, a test room measuring 24 cm x 26 cm x 1 m was constructed from plywood, as shown in Figure 2.3.6 and fixed to a plywood platform which was then mounted to the heliodon. The blinds frame was fixed to one end of the model, covering the single opening in the space. A track, holding 6 sensors was mounted to the ceiling and the sensors were placed at 14.3-cm intervals, starting at a distance of 3 cm from the window. In order to capture incident rays on the ceiling emitted at very low angles relative to the ceiling, the sensors were fixed to aluminum angle brackets, which were milled so that the sensor had a 45° tilt toward the blinds. The interior of the room and the sensor track and angle brackets were painted matte black. Exterior plywood surfaces "seen" by the blinds were covered with black velveteen to minimize exterior reflections, as were some unpainted metal bars on the heliodon itself. The only remaining reflective surfaces within view of the blinds were on the control computer and stand. These were covered by a large piece of black felt, and the operator sat under this curtain while making measurements.

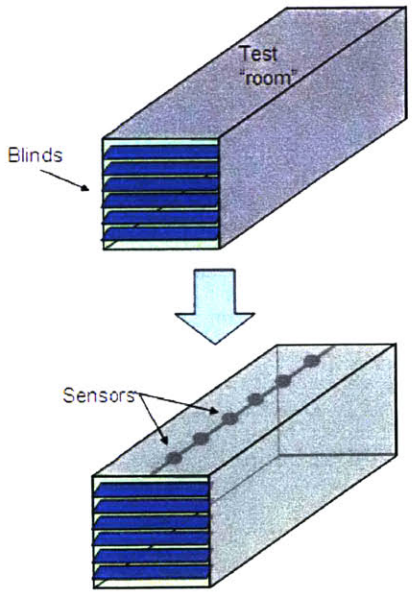

Figure 2.3.6 Schematic of model used in overcast sky simulations

Due to the relatively large dimension of the model, it was necessary to manipulate the control software so that the portion of the model extending beyond the edge of the heliodon bed would not interfere with the rotation of the heliodon. The path of travel of the test room was restricted to 180° and three measurement positions, instead of making the full 360° sweep to capture all six measurements. This did not affect data gathering, as the three measurements missed by restricting the path would be taken when the single opening of the model is facing away from the sky dome patch, and should not be receiving any light. In order to accommodate the pre-set path of the heliodon determined by the control software, the plywood platform was fixed to the heliodon so that the test room start position, position #1, was at -60° from the normal, position #2 was at the origin, and position #3 was at +60°. Figure 2.3.7 shows a schematic in plan view of the test setup and illustrates the three test positions.

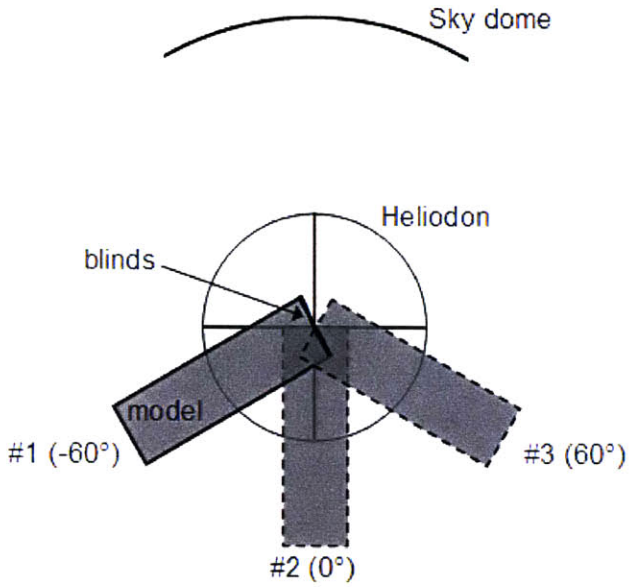

Figure 2.3.7 Plan view of three model test positions

2.4 Experimental Results: Surface Reflectances

Reflectance measurements were performed for all significant surfaces (black painted surfaces, white painted surfaces, glass mirror, aluminum mirror). Diffuse and average specular reflectance were measured against reference diffuse and specular surfaces, as appropriate. A diffuse white sample and a specular silicon wafer of known reflectivities were used as references. Both total and diffuse reflectance measurements were taken using an integrating sphere combined with a spectrophotometer. Compiled below are the reflectance coefficient values for the tested surfaces:

Table 2.4.1 Measured surface reflections for scale model components

Surface	Total Reflectance	Diffuse Component
White paint	91%	Not tested (~100%)
Black paint	2%	98%
Aluminum blind	99%	< 0.1%
Glass blind	97%	< 0.1%

Both the aluminum and the glass mirror are very close to purely specular (the specular component can be determined by subtracting the diffuse value from the total value measured with the integrating sphere). Both have reflectance coefficients close to unity. As a result, the numerical model assumption of a perfectly specular surface with an appropriate reflectance coefficient is likely sufficient. All reflectance measurements are subject to an error of ± 2%.

The painted black surface shows a total reflectance coefficient of 2%, with a specular component of 2%. The model was intended to be perfectly black, with the primary concern being the reflectance of the floor, in order to avoid reflection of the light passing directly through the blinds onto the floor. A 2% reflectance coefficient is low enough to assume a perfectly black model interior. This can be shown by calculating reflected light from the floor to the ceiling using configuration factors and a "one-bounce" theory. The calculated theoretical configuration factor from the floor to the ceiling is 0.44. Assuming

that the light that bounces off the floor, reflects off the walls, and then hits the ceiling is negligible, we can approximate the percentage of light hitting the floor that will be reflected to the ceiling

$$0.44 \times 2\% = 0.9\% \qquad (2.4.1)$$

This percentage corresponds to a value of roughly 0.05% daylight factor at most[1], which is within the error band of the measurements.

2.5 Experimental Results: Artificial Sky Simulations

Experimental testing of the scale model under the scanning sky simulator consisted of two phases. For the first, the inside of the model was painted black and the sensor track was positioned on the ceiling. This set of experiments was performed to validate both the accuracy of the numerical model and the optimization technique. For the second set of tests, the inside walls and ceiling of the model was painted white and the sensor track was fixed to the floor of the model (at the corresponding full-scale height of one meter, or workplane height, as defined in the numerical model). This configuration was designed to measure the workplane illuminance due to the illumination of the ceiling, which was not modeled numerically.

Error

All daylight factor measurements are subject to an error not greater than 25%. Experimentation has shown a relative discrepancy between theoretical and measured sky luminances under the simulator to be less than 1.5% for the isotropic overcast sky. (24)

---

[1] This calculation is based on measurements taken with the sensors placed on the floor and the model painted black, in order to capture only the light that passes through the blinds directly to the floor. A maximum of 5% daylight factor was measured with horizontal blinds in place and this was measured very close to the window opening. The illuminances measured farther back from the opening drop off very quickly.

The LMT luxmeters used in the experiment have been shown to exhibit cosine correction error +15% above the ideal cosine response. (18) Error due to reflectivity of the black model interior will be considered negligible, as shown in Section 2.4, and therefore will not be a significant source of error. An uncertainty in blind angle adjustment of 2° adds an error of less than 5% illuminance measurements.

Because of the large dimension of the model relative to the sky dome radius, measurements are potentially subject to a large parallax error, however this error is not applicable to this particular set of experiments. Under non-uniform skies, parallax error results from the fact that these sensors "see" a different luminance distribution compared with the luminance distribution that would be seen under the real sky when the sensors are place at significant distances from the center of the dome. For these experiments, the ratio of the sky dome radius to the largest model dimension is 2.5:1, less than the recommended model to sky dome ratio of 14:1 necessary for an error margin less than 25%. (25) Therefore, the sensors at the back of the model, 1 m from the heliodon center, should be subject to significant parallax error. However, the placement of the single model opening at the center of the heliodon and the fact that all tested sky simulations were isotropic simplifies the error. Because the isotropic sky is perfectly diffuse and uniform, it will present the same luminance distribution even when viewed from positions outside the center of the hemisphere.

As discussed in Section 2.3, the large dimensions of the model prevented the collection of data points at all six positions on the heliodon. As a result, only three measurements were taken, comprising half a hemisphere: one with the model positioned so that the opening faces the center of the sky dome segment (the three positions shown in Figure 2.3.6). The processing software for the sky simulator automatically calculates a daylight factor based on a measurement of six data points, and this artifact causes an over prediction of light levels by a factor of two. All data output from the heliodon is therefore corrected for this over prediction. In the cases in which a measurement consisted of only one position, this data point was corrected by a factor of 6. This was confirmed by Professor Jean-Louis Scartezzini, director of LESO-PB at EPFL.

Additionally, in order to compare the data with the numerical model which predicts the illuminance on the horizontal ceiling plane, it is necessary to make an adjustment to data taken with sensors oriented at 45°. This is accomplished by projecting the values measured by the sensors onto the horizontal plane of the ceiling. This adjustment method assumes that all incident angles to the ceiling are less than 45°. This adjustment may not be an appropriate assumption for measurements taken close to the window, as the incident angle to the ceiling for some rays is greater than 45° and this would cause over-prediction of actual values. However, the primary aim of these experiments is to determine the lighting conditions at distances relatively far from the window, and the approximation holds for distances farther from the window.

Experimental Results and Discussion

Initially, the model was tested with all the blinds in the horizontal position. Figure 2.5.1 and Figure 2.5.2 show the comparison between numerical prediction and experimental results for this simple case under an isotropic overcast sky. The measured quantity, illuminance ratio, is the ratio of the measured illuminance value at the ceiling to a reference global horizontal illuminance, measured outside the model. This quantity is often referred to as the "daylight factor" when the indoor illuminance measurement is taken at the workplane or at another surface of interest for occupant visual comfort. Because the illuminance ratio at the back of the room is relatively small for this case, an expanded graph showing only the lower range of illuminance ratio values is also shown.

The model shows poor agreement with the data points close to the window, under predicting by actual values by 40% at a distance of 0.3 m and over predicting by 20 - 30% at distances of 1.7 and 3.2 m (relative to full-scale model). However, model predictions for distances greater than 4.5 m show a strong correlation with experimental data, with discrepancies in the range of 5 - 10%. The wide disparity between measured and predicted values at the front of the room can be explained by two factors. First, the cosine adjustment for the 45° sensor orientation introduces error because the incident angles to the ceiling are greater than 45°. Under this approximation, the model would tend to over predict values.

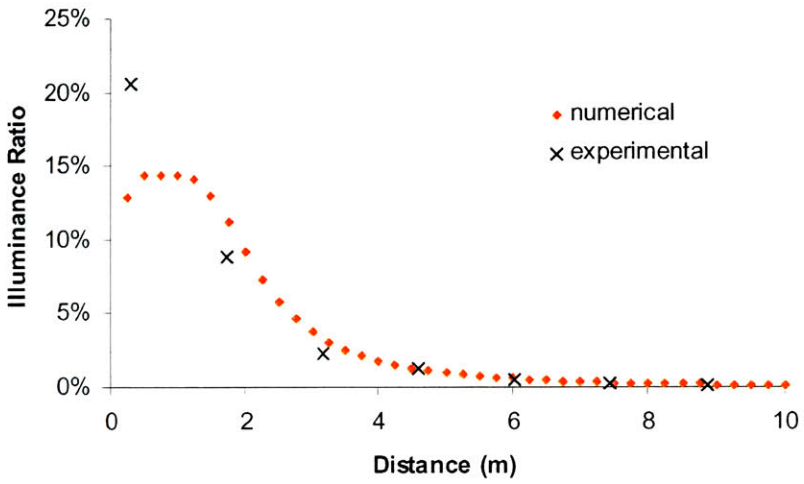

Figure 2.5.1 Ceiling illuminance ratio as a function of distance from the window for a horizontal blind configuration, measured in a black model. Distances scaled to the full-size room.

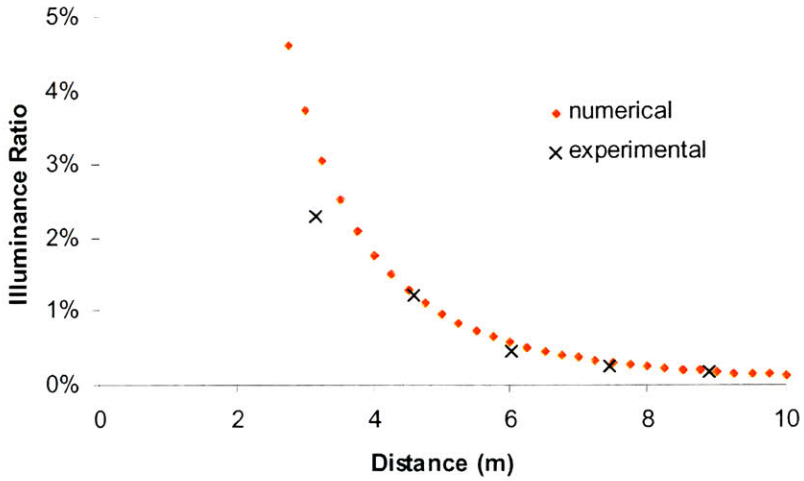

Figure 2.5.2 Ceiling illuminance ratio as a function of distance from the window for a horizontal blind configuration, measured in a black model, expanded

Second, the model is based on the assumption of a two-dimensional sky plane. This assumption could be approximated for the physical model by lighting only a single

vertical row of lamps on the sky dome so that the only light entering the blinds would be from an azimuth angle of zero, or from the normal direction. Instead, as tested under the sky dome, the blinds receive light from a 180° azimuth range. The sensors at the back of the model do not have a direct line of sight to the portions of the sky dome at wide azimuth angles and the light from these angles that is reflected into the model by the blinds is absorbed by the black interior of the model and does not reach the back of the model. Therefore, the two-dimensional approximation holds for points at the back of the room, as the azimuth angle of the sky dome seen by the sensor is small and the sensor receives light only from a small range of angles. However, the sensors close to the blinds will receive light from both sides, in addition to from the normal direction, and so the two-dimensional assumption will tend to under predict light levels at distances close to the blinds.

In order to test the validity of the latter source of discrepancy, the experimental procedure was modified so that measurements within the model were taken only in the normal position relative to the sky dome lamps. Figure 2.5.3 shows this comparison between the test under the full hemisphere, and the test under only the normal portion of the sky dome. Although all lamps within the center $1/6^{th}$ of the hemisphere were lit (not only the single vertical line normal to the model), this experiment provides sufficient evidence to confirm that the three-dimensional nature of the experimental model contributes significantly to light levels at the front of the room, but not to the back of the room. As a result, the closest measurements to the window will not be considered.

The optimal blind configuration for maximum ceiling illumination at the rear of the room determined from the numerical model was also tested under an isotropic overcast sky simulation. In order to confirm the model prediction that ceiling illumination at the rear of the room is not highly sensitive to optimization of individual blind angle, two different optimized configurations were tested: one with all blinds optimized to a single angle, and another with each blind optimized to a unique angle. Experiment confirmed the model prediction, with daylight factor values at the back of the room varying by negligible amounts between the two configurations, as seen in Figure 2.5.4. Measured values for these optimized cases are lower than the model-predicted values, with the model over

predicting by 10 - 30%, yet these values are not far outside the error range for the experiments.

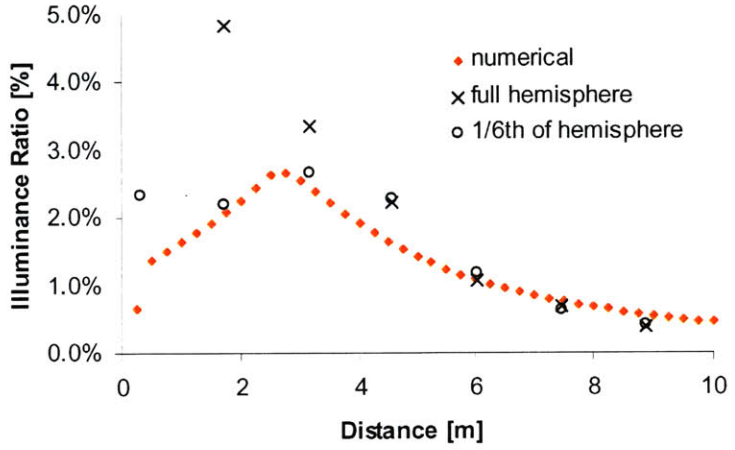

Figure 2.5.3 Ceiling illuminance ratio as a function of distance under varying sky dome sections

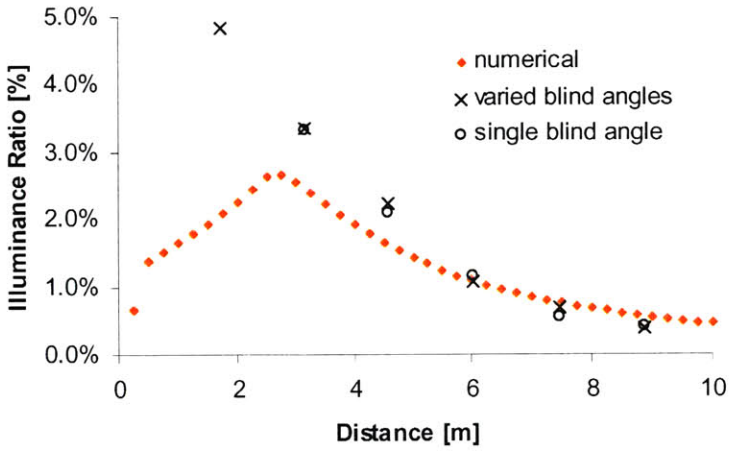

Figure 2.5.4 Illuminance ratio as a function of distance, comparing numerical model with experimental data taken for optimized configurations within a black model

In order to test the impact of the blinds on the workplane, the inside of the model except the floor was painted white (reflection coefficient, 91%) and the sensor track was placed on the floor of the model, representing a workplane height of 1 m in a 3-m room with blinds covering the top 2/3 of the opening. Additionally, the sensors were rotated to the horizontal position, in order to accurately measure absolute values of horizontal workplane illuminance. For these tests, the same illuminance ratio is measured, but in this case it will be referred to as "daylight factor," as it describes the ratio of interior illuminance measured at the workplane to exterior global horizontal illuminance. The model was tested under isotropic sky conditions for three cases: no blinds (uncovered window reference), horizontal blind position, and optimized blind positions. These experiments captured the complex inter-reflections between the ceiling, walls, and back of the room that were not modeled numerically. Figure 2.5.5 shows that the horizontal blind configuration yields a moderate increase in illuminance distribution over the uncovered window; however, this improvement decreases farther back in the room from a 30% increase at 4.6 m to only an 11% increase at 8.9 m. The daylight factor measured at the rear of the room is 1.2% for the uncovered window, little over half the required minimum daylight factor of 2.0% for office lighting conditions. To quantify the contribution of light from the sky dome passing directly through the blinds onto the sensors (isolating this component from the effects of inter-reflections on the white interior), a test was also conducted for an uncovered window with the sensors at the workplane level, but with the interior painted black. These results, given in Figure 2.5.6, show that this component is small (less than 0.3% daylight factor for measurements beyond 5 m) compared with measured daylight factors for various blind configurations in a white interior, suggesting that the bulk of the illuminance seen by the sensors is due to light reflected to the ceiling by the blinds.

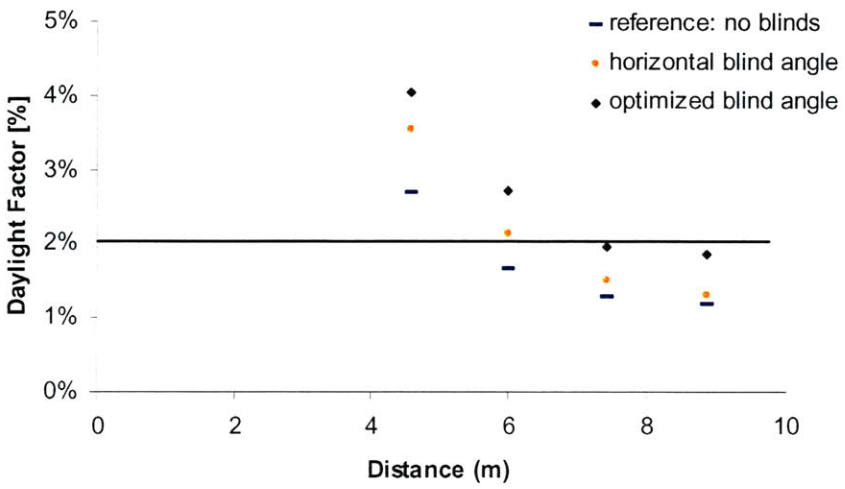

Figure 2.5.5 Daylight factor as a function of distance from window, measured at the workplane for various blind configurations under an isotropic overcast sky, within a white model (ρ = 91%)

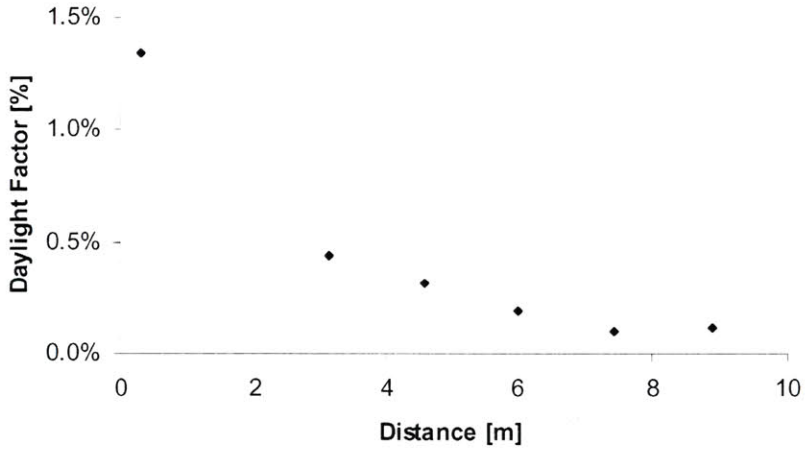

Figure 2.5.6 Daylight factor as a function of distance due to light transmitting directly through the blinds to the workplane, measured at the workplane within a black model with blinds in the optimized position

Also shown on the graph in Figure 2.5.7 are interior daylight factor values for the simulation in which the blinds are positioned to the optimized angle for maximum ceiling

illuminance at 10 m. Daylight factor at the rear of the room is increased by 50 – 60% at distances of 4.6 m – 8.9 m from the window with the addition of the blinds in the optimized configuration of 21°. Interpolation of the data show that sufficient lighting conditions (2% daylight factor) can be achieved to a distance of 7 m. Though the daylight factor falls just short of 2% at distances beyond this, the blinds system nevertheless provides a significant increase in the light level, as compared with the reference case.

In addition to testing the agreement between model and experimental results, experiments were conducted to confirm that the predicted optimal configuration did indeed provide maximum illuminance to the workplane at the back of the room. Inward facing blind angle configurations of 10°, 15°, and 25° around the predicted optimal configuration of 21° were tested. Figure 2.5.7 shows the results from these tests at a distance of 7.5 m (scale is adjusted to magnify small differences). The predicted optimal blind angle, 21° inward, does in fact provide maximum daylight factor to the rear of the room. However, it does so by only 0.1% daylight factor, compared with the scenarios tested at ±5° the optimal configuration, showing that daylight factor is not highly sensitive to angle adjustments of smaller increments at configurations close to optimal.

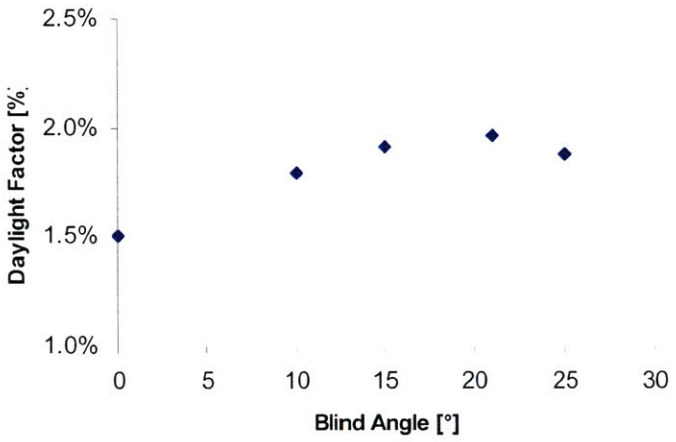

Figure 2.5.7 Daylight factor as a function of blind angle for suboptimal configurations, compared with optimal setting at 21°, measured at the workplane at a distance of 7.5 m from the window, within a white model (ρ = 91%)

3 Blind System Performance: Direct Solar Incidence

3.1 Numerical Modeling for Direct Solar Incidence

In order to model the blinds' response to direct sun, the sky is assumed to provide only a direct component of radiation to the façade (a reasonable assumption, as the light added by the diffuse sky component is small compared to the direct component). The blinds are assumed to have no diffuse component and the perfectly black lower surface of the blinds eliminates any blind-blind reflections. Therefore, the light reflected into the space undergoes only one reflection, which is purely specular. The sun is taken as a collimated source and is reflected off each flat blind to the ceiling. Geometric ray tracing, taking into account blind angle and angle of the blind immediately above, yields the position and intensity of light redirected to the ceiling, as well as light that is directly transmitted through the blinds. The initial portion of the analysis assumes a sun azimuth angle of 0°.

The blind plane receives a flux per unit area (the model assumes a direct solar illuminance of 100 klux, or 100,000 lumens/m^2, measured normal to the sun's rays for a clear sunny day). From this incident illuminance and the projected area of each blind normal to the incident rays, the incident flux on the blinds can be calculated. Of this incident light, a fraction passes directly through the blinds to the floor of the model, without undergoing any reflections. The remaining light is intercepted by the reflective upper surface of the blind. This light may be reflected to the ceiling, reflected to and absorbed by the black lower surface of the blind immediately above, or reflected back outside, depending on the incident solar angle and the orientation of the blinds. For modeling purposes, the upper surfaces of the blinds will have a reflection coefficient of 95%. This value will serve as a more conservative estimate of achievable blind reflectances and is slightly lower than measured values for tested materials.

The light that is reflected to the ceiling forms horizontal beams of light that run parallel to the façade. The flux within each beam is determined by the incident angle of the sun, the angle of the blind, and the masking effect of the blind above. The model calculates the percentage of incident flux that is reflected by the blind surface in lumens. This quantity, adjusted for the reflection coefficient of the blind surface, is the flux that the ceiling will receive within the horizontal beam. This incident flux on the ceiling is divided by the total area of the reflected beam on the ceiling, yielding the illuminance on the ceiling.

In order to create sufficient illuminance levels throughout the space, the model calculates the optimal blind angle to evenly distribute the light redirected to the ceiling by the blinds over a distance of 10 m from the window, for a given incident solar angle. Figure 3.1.1 shows a schematic of the intended redirection pattern.

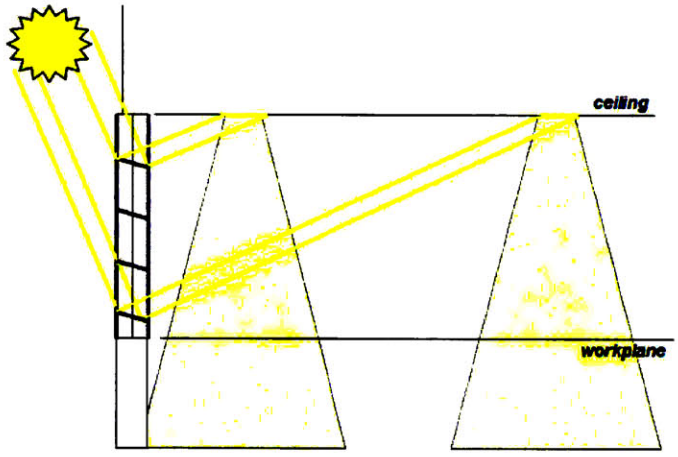

Figure 3.1.1 Schematic of light distribution based on blind redirection

The model attempts to tune the blinds in order to evenly distribute redirected light over the 10-meter depth of the ceiling. This distribution is accomplished if the angle that the rays exit the blinds is held constant by varying the blind angle in response to changing solar altitude, so that the redirected ray from the lowest blind is always centered at the desired penetration distance from the window. For a 10-m deep space, with a window of

height 2 m, the rays should exit the blind at an angle of approximately 11.3° above the horizontal, as calculated in Equation (3.1.1). From this target redirection angle, the blind angle can be calculated from the geometrical relationship between incident solar angle, β, blind angle, θ, and exiting redirection angle, α. Figure 3.1.2 shows these angles for an incident solar ray from the left, redirected to the right, with positive angles in the clockwise direction, and Equation (3.1.2) gives the exit angle as a function of incident and blind angles .

$$\alpha = 90° - \arctan\left(\frac{10m}{2m}\right) = 11.3° \qquad (3.1.1)$$

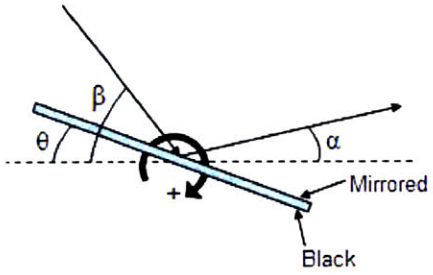

Figure 3.1.2 Angle reference and convention

$$\alpha = -\beta + 2\theta \qquad (3.1.2)$$

Based on these calculations, the blind angle for optimal light redirection can be calculated for a range of incident angles, as shown in Table 3.1.1. Except for the lowest incident solar angles, the optimal angle is positive, that is, the reflective side of the blind tilts in toward the interior.

However, as discussed in Section 1.3, the primary design goal is the prevention of direct solar transmission onto the workplane when considering a façade that receives direct solar incidence, in order to prevent visual and thermal discomfort for occupants. To

accomplish this, the blinds must be angled toward the direction of solar incidence (for a system in which all blinds are at the same angle), so that all solar radiation is either reflected to the ceiling, reflected to and absorbed by the black underneath surface of the

Table 3.1.1 Optimal redirecting blind angles for given incident solar angles

Incident solar angle	5°	10°	15°	20°	25°	30°	35°	40°	45	50°
Redirecting blind angle	-3.2°	-0.7°	1.9°	4.4°	6.9°	9.4°	11.8°	14.3°	16.8	19.3°

Incident solar angle	55°	60°	65°	70°	75°	80°
Redirecting blind angle	21.8°	24.3°	26.8°	29.3°	31.8°	34.3°

blinds, or reflected back outside. The negative angles necessary to provide adequate shading of direct transmission are at odds with the positive preferred angles for light redirection, and therefore prevent light redirection to any meaningful depth. Figure 3.1.3 and Figure 3.1.4 show transmission and reflection responses for these two cases.

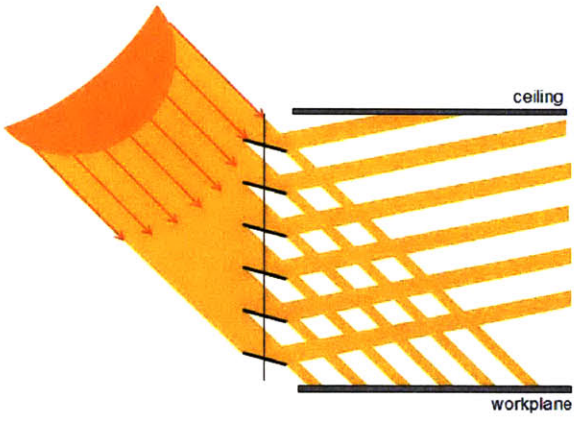

Figure 3.1.3 Blinds optimized for sunlight redirection

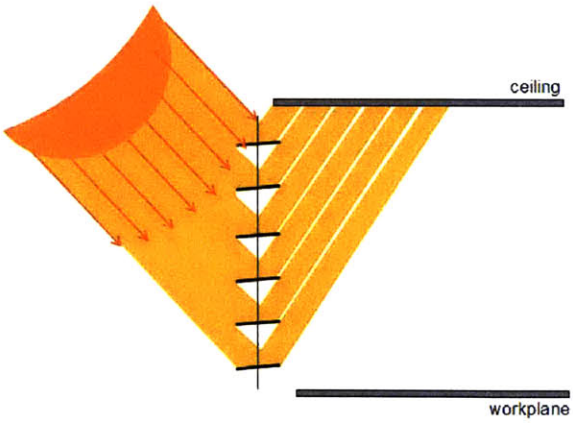

Figure 3.1.4 Blinds optimized for sunlight shading

An alternative configuration uses varying blind angles to achieve both shading and sufficient light redirection, using alternating blinds to redirect and block direct transmission as shown in Figure 3.1.5. This arrangement sets every even-numbered blind,

called reflecting or *R* blinds in this thesis for identification purposes, to the optimal angle for redirection according to Equation (3.1.2). The odd numbered blinds, shading or *S* blinds, are then adjusted in the direction of the incident rays to provide shading until direct transmission is just blocked. Equation (3.1.3) gives the relationship, when combined with Equation (3.1.2), between angles θ_S and θ_R of the *S* and *R* blinds and incident angle, β, that allows maximum sunlight redirection while providing just enough shading so as to prevent direct transmission.

$$\cos(\beta) = \frac{1}{2}\left[\sin(|\theta_S - \beta|) + \sin(|\theta_R - \beta|)\right] \qquad (3.1.3)$$

Although redirection to the desired distance of 10 m can be achieved for a larger range of incident angles using this scheme, the number of blinds contributing to the redirection of light at the optimal angle of 11.3° is reduced by half.

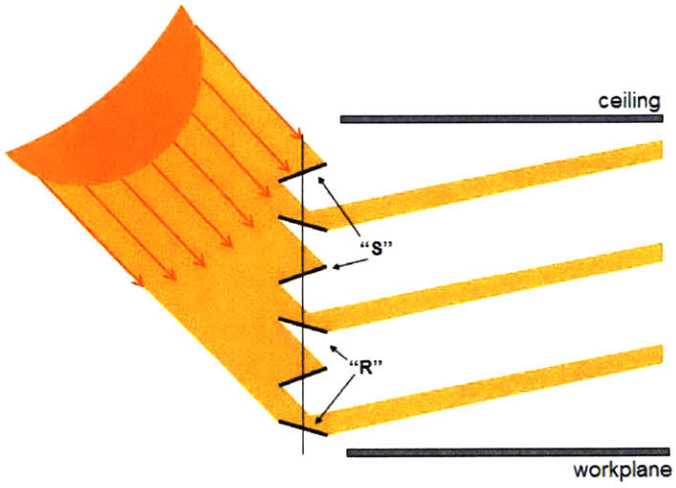

Figure 3.1.5 Blinds configured for combined function, showing both redirection blinds, type *R*, and shading blinds, type *S*

Depending on the incident solar angle and the required shading blind angle, the *S* blinds will either direct light inside toward the ceiling close to the window or toward the

outside. If the required angle of the shading blind is such that it redirects light to the ceiling close to the window, an unequal ceiling light distribution is created with a higher illuminance near the window, which may cause sub-optimal lighting conditions. However, this negative effect must be weighed against the benefit of increased lighting at the rear of the room in order to evaluate the overall effectiveness of the daylighting system.

Table 3.1.2 gives the optimal angle configuration for this alternate scheme over a range of incident angles. Efficiencies include losses due to a 95% blind reflection coefficient.

Table 3.1.2 Optimal configurations for incident solar angles ranging from 10° to 80° for shading/redirecting scheme

Incident Solar Angle	Optimal Angle: *R* Blinds[1]	Best Allowable Angle: *R* Blinds	*S* Blind Angle	% of Incident Radiation Redirected	Penetration Depth [m]
10° [2]	-1°	NA	NA	NA	NA
15°	2°	NA	NA	NA	NA
20°	4°	NA	NA	NA	NA
25°	7°	-30°	-65°	43%	0.17
30°	9°	-17°	-60°	40%	1.0
35°	12°	-5°	-55°	37%	2.0
40°	14°	7°	-50°	33%	4.1
45°	17°	17°	-26°	31%	10.3
50°	19°	19°	-2°	37%	9.4
55°	22°	22°	18°	45%	10.3
60°	24°	24°	24°	95% [3]	9.4
65°	27°	27°	27°	95%	10.3
70°	29°	29°	29°	95%	9.4
75°	32°	32°	32°	95%	10.3
80°	34°	34°	34°	95%	9.4

[1] All angles rounded to nearest degree.

[2] Not possible to redirect incident rays lower than 25° without allowing some directly transmitted light.

[3] The redirecting blind angle for incident rays 60° and greater provides sufficient shading, so all blinds may be set to the redirecting angle.

For incident solar angles lower than 44° altitude, it is not possible to achieve redirection to a distance of 10 m while still preventing direct penetration. For incident angles lower than 25°, it is not possible to achieve redirection of light to any distance within the space without allowing penetration. Figure 3.1.6 demonstrates this phenomenon for an incident angle of 25°. The lower, or redirecting, blind is set to the optimal angle for redirection to 10 m, while the upper blind is set to the best possible angle for shading an incident solar angle of 25° (perpendicular to the incoming rays). In this configuration, a good portion of the solar rays are directly transmitted, and so the redirection angle must be modified, yielding a maximum penetration of far less than 10 m. This modified configuration for a 25° solar altitude limits the maximum distance for redirection to a distance of 0.2 m from the window, as shown in Figure 3.1.7.

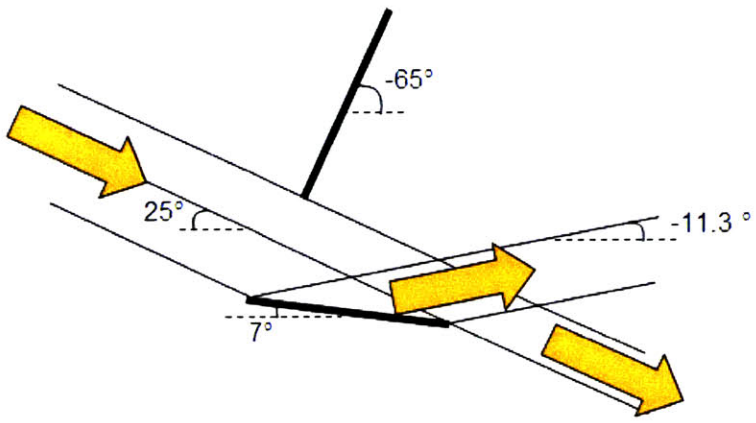

Figure 3.1.6 Optimal redirection angles for low incident solar angles allows direct transmission

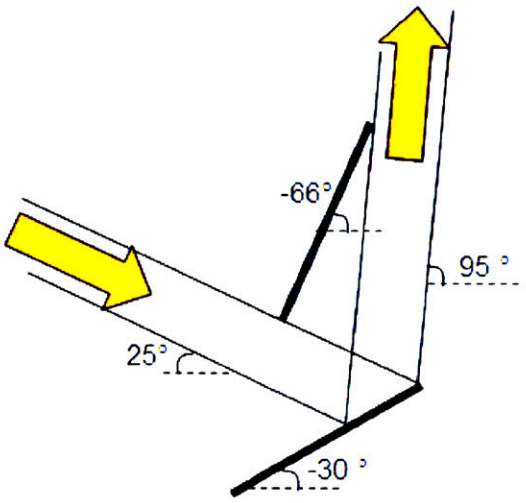

Figure 3.1.7 Optimal shading angles for low incident angles prevent significant redirection in penetration depth

At incident angles above 44°, it is possible to position the blinds to shade all direct transmission, yet redirect light so that it exits the blind at the 11.3° angle necessary to reach a distance of 10m. Figure 3.1.8 shows this optimal configuration for an incident angle of 45°.

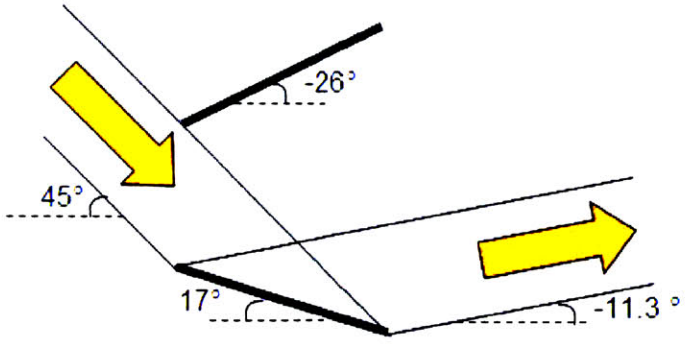

Figure 3.1.8 Optimal configuration for 45° incident solar angle, meeting both shading and redirection requirements

Above an incident solar angle of 60°, the blind angle necessary for redirection provides sufficient shading, and all blinds are set to this angle in order to maximize the view through the blinds, as shown in Figure 3.1.9. For these cases, because both shading and redirecting blinds may be used, all incident light is redirected at the optimal exit angle of 11.3°.

As demonstrated, this blinds configuration scheme is fully effective only when the solar altitude is greater than 45°. This greatly reduces the effectiveness of a daylighting system, as it largely limits usage to the southern façade because east- and west-facing facades rarely experience solar angles greater than 45°, except for equatorial locations. In addition, the system is limited to use only during summer months for many locations. In Boston, for example, the system would provide sufficient lighting to 10 m at noon on the southern façade for only 6 months out of the year.

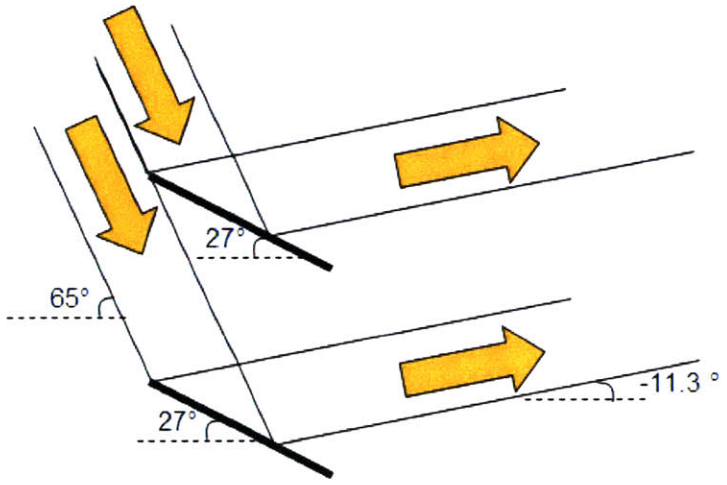

Figure 3.1.9 Optimal configuration for 65° incident solar angle

Optimization: Multiple Blind Reflections

This combined shading/redirecting configuration was tested for a sample of incident angles using a physical scale model, as described in Section 3.3. Access to testing facilities was limited; therefore only this initial configuration was physically tested.

However, agreement between numerical model and experimental results confirmed the numerical model and allowed further investigation using only the numerical simulation. A third possible configuration uses the underside of the *S* blinds for redirection. For this configuration, the *S* blinds are rotated 180° so that the mirrored side faces down and the black side faces up. The redirecting blind is oriented to reflect incident light to the underside of the above shading blind, which is tuned to reflect the light at an exit angle of 11.3°. Examples of this configuration for incident angles of 10°, 25°, 45°, and 65° can be seen in Figure 3.1.10.

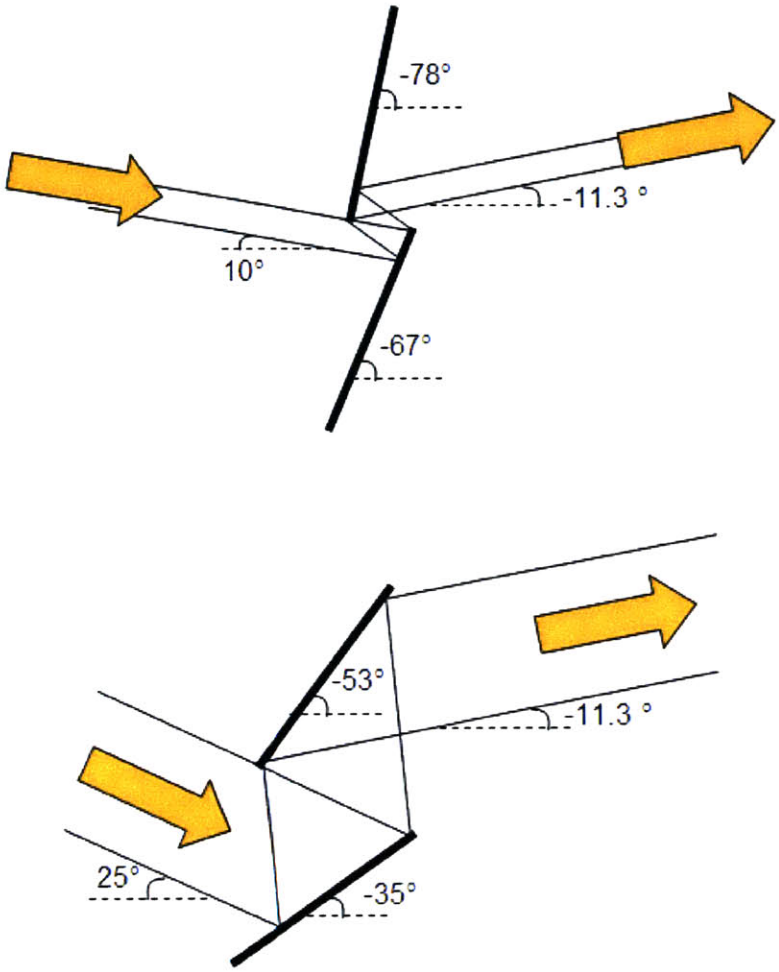

Figure 3.1.10 Optimal configurations for 10°, 25°, 45°, and 65° incident solar angles

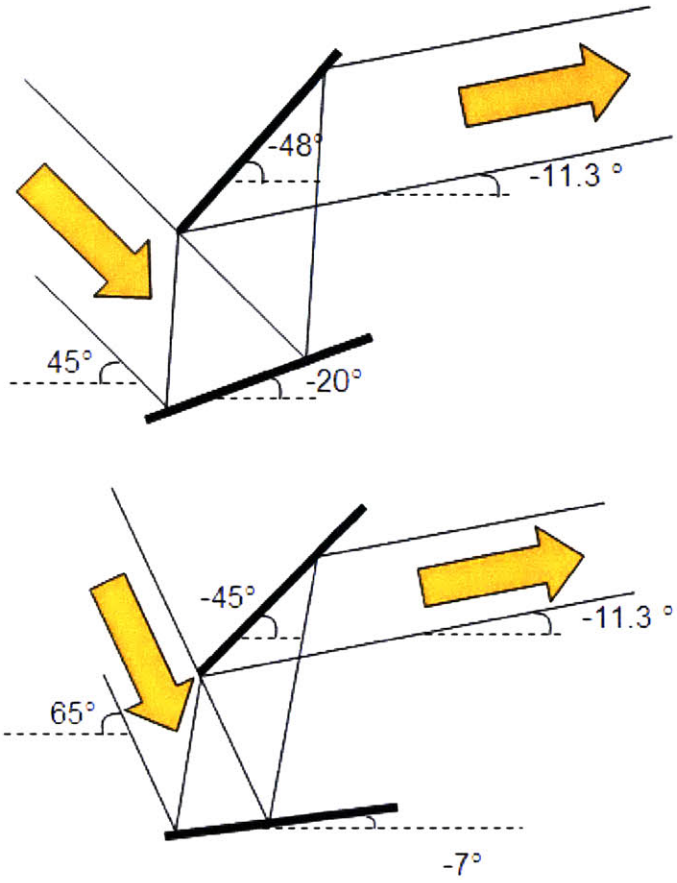

Figure 3.1.10 (cont'd.) Optimal configurations for 10°, 25°, 45°, and 65° incident solar angles

By using multiple reflections, it is possible to redirect light deep into the space for a larger range of incident solar angles, as compared with the method previously discussed. Table 3.1.3 shows the optimal angles for this configuration (blind reflectivity = 95%). A light redirection depth of 10 m is possible for all incident solar angles. The fifth column provides a comparison of efficiencies with the previous configuration. For incident angles lower than 25°, this configuration allows a fraction of light (albeit small) to be redirected to 10 m while still providing adequate shading of direct transmission. Compared to the

previous configuration which was unable to redirect any light at low solar angles, the current scheme is preferable. For the range of incident angles from 25° to 45°, the current scheme allows the same or a slightly greater amount of light to enter the space, but achieves the desired penetration depth of 10 m, while the previous configuration does not allow such depth of light distribution. The two systems are comparable at a 50° incident angle, and the single-reflection system slightly outperforms for an incident angle of 55°. For solar angles greater than 60°, the previously discussed uniform angle scheme allows 100% of incident light to be redirected into the space (dedicated shading blinds are no longer required), and so this scheme is preferable under these conditions.

A negative consequence of the latter system is the introduction of an additional reflection, further reducing the flux of the light redirected into the space by a percentage equivalent to the absorption coefficient of the mirror material. Combining the strengths of both systems, an optimal operational program would use the single-reflection scheme for incident angles greater than 45° and the double-reflection scheme for angles less than 45°.

Predicted Workplane Illuminance Levels

Because the ultimate goal is regulation of the illumination on the workplane, it is necessary to evaluate this configuration based on the illuminance it provides to surfaces below. To do this, the model employs the same crossed-strings configuration factor method as used for the study of the blinds' response to the diffuse sky, as discussed in Section 2.2. Each blind slat reflects one "band" of light to the ceiling. This light band is considered to receive uniform illuminance, and to have known boundaries determined by geometrical ray tracing. The configuration factor is calculated between this band on the ceiling, and a workplane segment, 0.5 m in length. The configuration factor is calculated between all light bands and workplane segments, and the contributions to each segment are added to give the total illuminance on each workplane segment. Because calculation of daylight factor is relevant only for overcast sky conditions, this metric can not be used in this case. Absolute values of workplane illuminance will be used to evaluate the efficiency of each configuration.

Table 3.1.3 Optimal configurations for incident solar angles ranging from 10° to 80° for double-reflection scheme

Incident Solar Angle	*R* Blind Angle	*S* Blind Angle	% Incident Radiation Redirected	*% Incident Radiation Redirected (single-reflection scheme, reproduced from Table 3.1.2)*
10°	-67°	-78°	6%	*NA*
15°	-55°	-68°	13%	*NA*
20°	-44°	-60°	22%	*NA*
25°	-35°	-53°	30%	*43%*
30°	-31°	-52°	30%	*40%*
35°	-28°	-51°	31%	*37%*
40°	-24°	-50°	32%	*33%*
45°	-20°	-48°	34%	*31%*
50°	-16°	-47°	36%	*37%*
55°	-12°	-45°	38%	*45%*
60°	-9°	-45°	39%	*95%*
65°	-7°	-45°	41%	*95%*
70°	-4°	-45°	44%	*95%*
75°	-1°	-44°	48%	*95%*
80°	2°	-44°	58%	*95%*

Figure 3.1.11 shows the illuminance distribution along the workplane for an incident angle of 45°, using the dual-reflection system (blind reflectivity = 95%, ceiling reflectivity = 90%). The distribution curve is fairly flat (within 10% of maximum value) between 3 and 8.5 meters and exhibits a factor of difference of only 1.4 between minimum and maximum values (at 10 and 5 m, respectively). Illumination levels fall just short of the minimum recommended illuminance level of 400 lux for office desk work. Distribution curves for each of the blind angle configurations exhibit similar shape, adjusted in amplitude by the changing incident flux on the ceiling for the different cases.

Figure 3.1.12 gives the average illuminance at distances of 5 m and 10 m along the workplane as a function of incident solar angle for the range of incident angles. Note that workplane illuminances may differ for configurations with the same percentage of

transmitted light, as the available incident flux on the window decreases with the cosine of the incident angle.

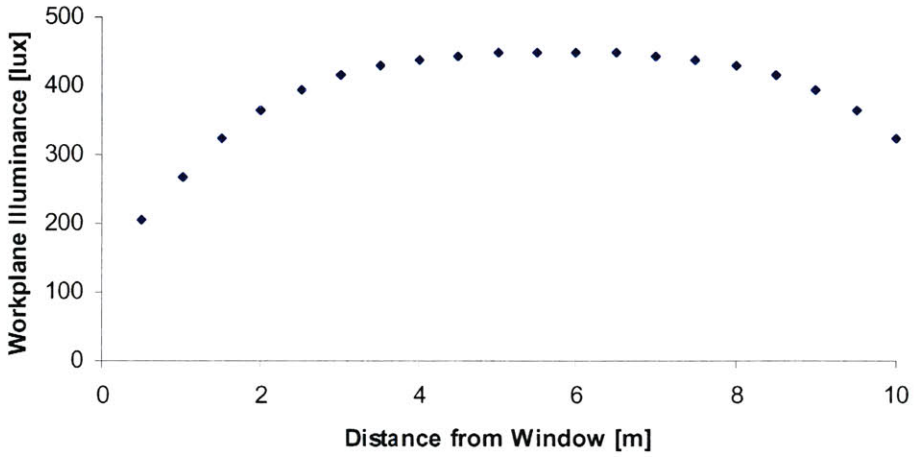

Figure 3.1.11 Workplane illuminance distribution as a function of distance for a 45° incident solar angle with a direct normal illuminance of 100 klux, using double-reflection configuration

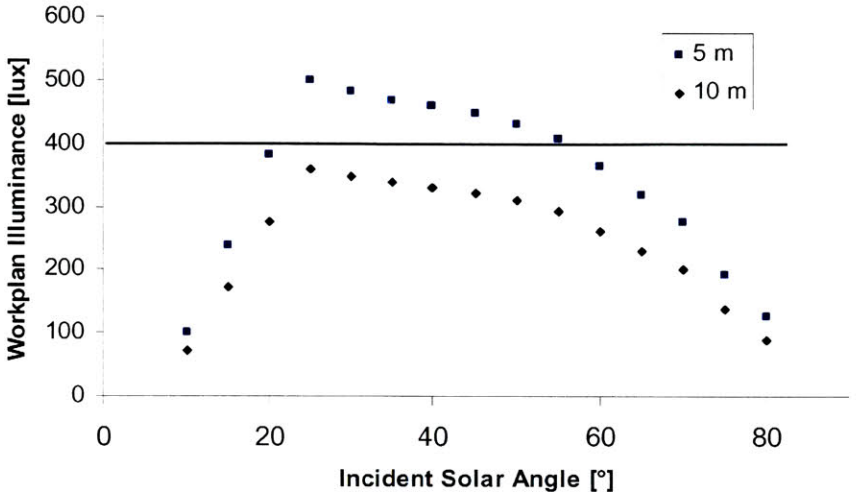

Figure 3.1.12 Workplane illuminance, as measured at 5 and 10 m from window, versus incident solar angle for double-reflection configuration

For incident angles between 25° and 55°, the double-reflection blind configuration provides sufficient illuminance levels of 400 to 500 lux for a good portion of the space, but fails to sufficiently light the workplane at the rear of the room. For the remaining incident angles, the system fails to provide sufficient lighting even at 5m. Therefore, it is preferable to modify the system to increase the total reflected flux to the ceiling.

Impact of Blind Spacing

A variety of modifications to the blind geometry would aid in shading and provide the desired increase in flux, including shifting the pivot point of the redirecting blinds out of line with the pivot point of the shading blinds, and adding a second layer of blinds behind the first. However, the optimal solution would increase the flux without requiring a design and fabrication process more complex than that of standard Venetian blinds. By decreasing the spacing of the blinds to allow some overlap, it is possible to reduce the slope of the blinds required for shading, thereby increasing the capacity to redirect light. Because, as shown previously in Table 3.1.3, the double-reflection configuration performs the worst for the lowest incident solar angles, the spacing adjustment should be optimized for low angles, granted that the modification does not adversely affect

performance at higher solar angles. Within these constraints, spacing should be kept to a maximum in order to preserve view to the outside. Figure 3.1.13 shows a comparison among configurations with varying blind spacing for an incident solar angle of 10°.

The maximum percentage of flux that may be redirected to the ceiling for an incident angle of 10° is shown in Figure 3.1.14 as a function of spacing. The percentage of flux increases rapidly by reducing the spacing from 100% of the blind width to 80%, but little is gained by further reducing the spacing. As shown in Table 3.1.4, a spacing of 80% allows for nearly a six-fold increase in transmitted light for the lowest incident angles. For mid-range incident angles, there is a slight decrease in efficiency (less than 5%). Recalculated workplane illuminances for 5 m and 10 m for the 80% spacing are shown in Figure 3.1.15. Appendix B gives the full workplane illuminance distribution functions for various incident solar angles.

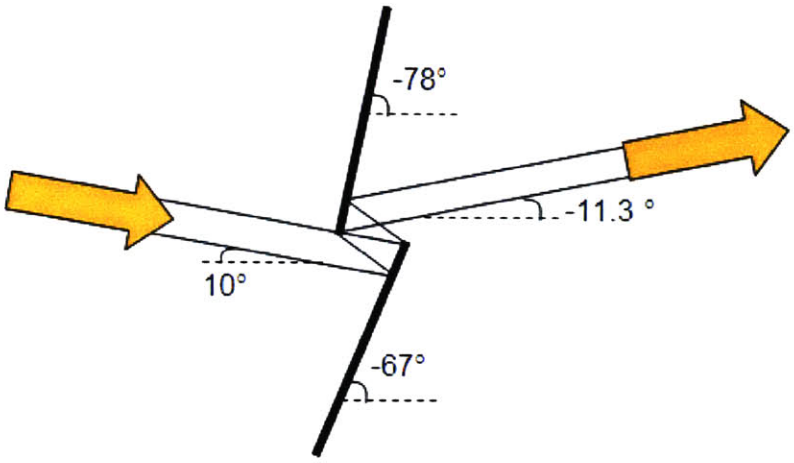

100% blind spacing, blind spacing = blind width

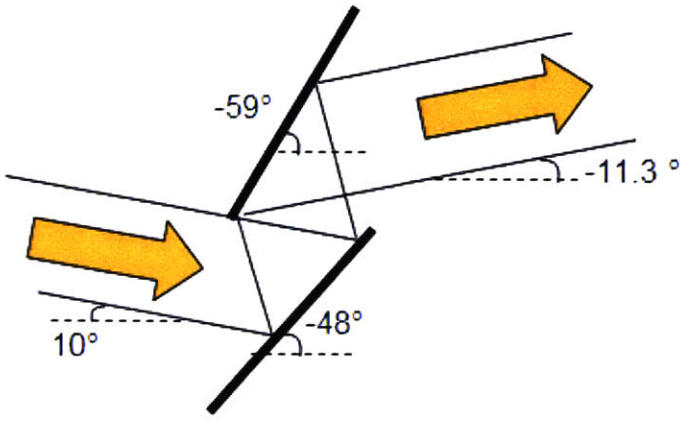

90% spacing (10% blind overlap)

Figure 3.1.13 Blind angle configurations of varying spacing for an incident angle of 10°

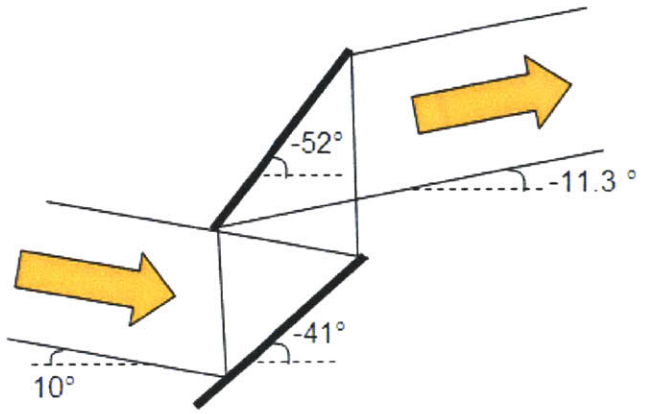

80% spacing (20% blind overlap)

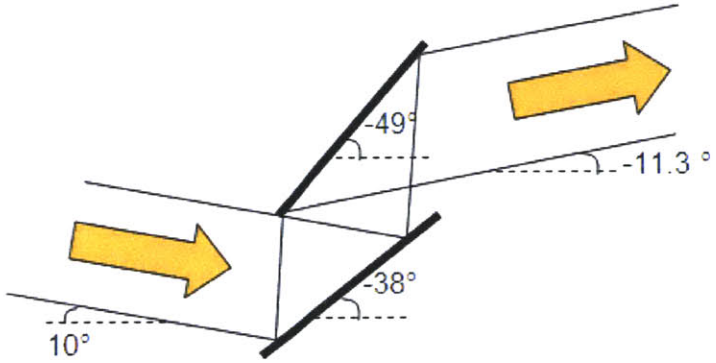

70% spacing (30% blind overlap)

3.1.13(cont'd.) Blind angle configurations of varying spacing for an incident angle of 10°

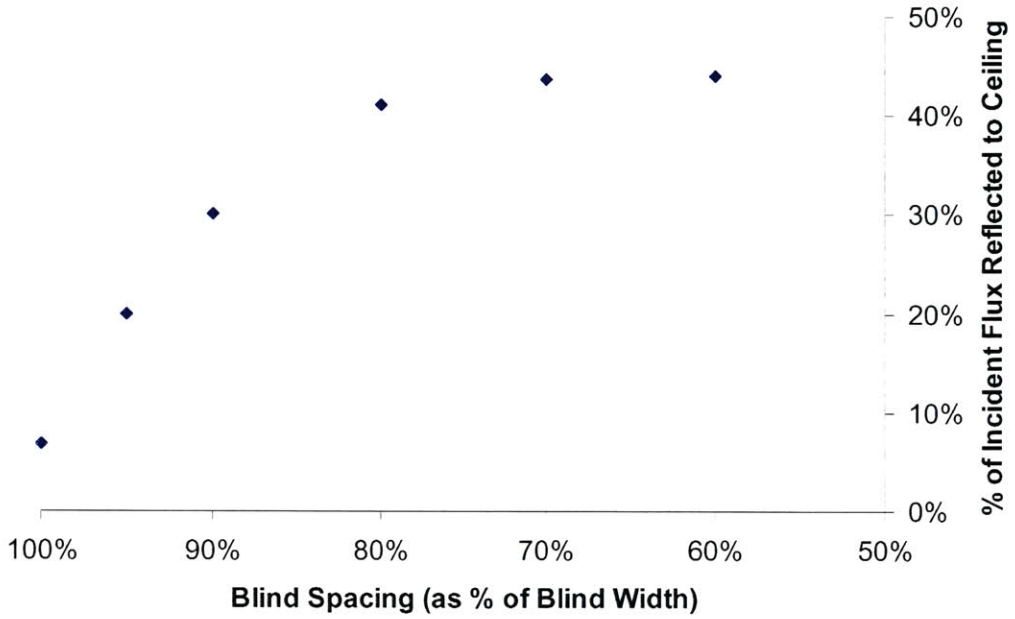

Figure 3.1.14 Reflected flux to ceiling as a function of blind separation for an incident angle of 10° using double-reflection configuration

Table 3.1.4 Optimal configurations for incident solar angles ranging from 10° to 80° with a blind spacing of 80% (overlap of 20%)

Incident Solar Angle	*R* Blind Angle	*S* Blind Angle	% of Incident Radiation Redirected	*% of Incident Radiation Redirected (100% spacing, reproduced from Table 1.2.3)*
10°	-41°	-52°	33%	*6%*
15°	-37°	-50°	33%	*13%*
20°	-50°	-34°	33%	*22%*
25°	-30°	-48°	34%	*30%*
30°	-27°	-48°	34%	*30%*
35°	-24°	-47°	34%	*31%*
40°	-20°	-46°	35%	*32%*
45°	-16°	-44°	36%	*34%*
50°	-14°	-45°	36%	*36%*
55°	-11°	-44°	37%	*38%*
60°	-8°	-44°	38%	*39%*
65°	-5°	-43°	40%	*41%*
70°	-2°	-43°	43%	*44%*
75°	1°	-42°	48%	*48%*
80°	3°	-43°	58%	*58%*

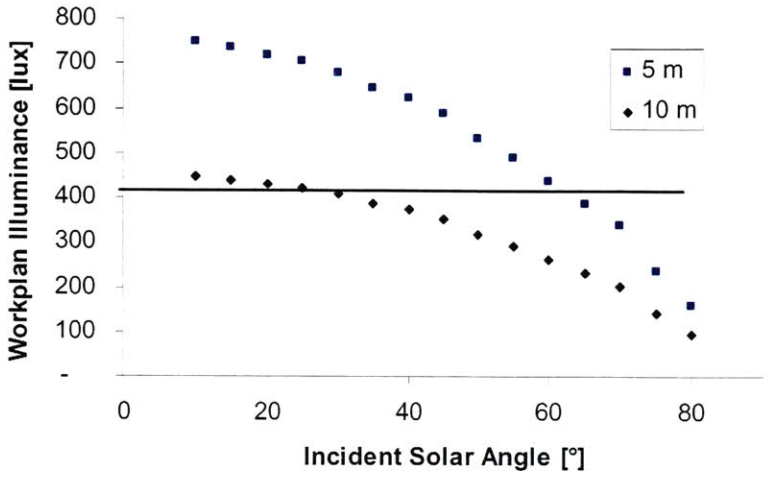

Figure 3.1.15 Workplane illuminance as a function of incident solar angle, measured at 5 and 10 m from window with a blind overlap of 20% for double-reflection configuration

The optimal configuration with a 20% blind overlap provides sufficient illuminance to the entire workplane for incident angles below 35° and sufficient illuminance to the workplane at a distance of 5 m from the window for all incident angles below 65°. Applying this spacing modification to the single-reflection model, the minimum incident solar angle that does not require separate shading blinds to prevent direct transmission (i.e. when both *S* and *R* blinds may be used for redirection) reduces to 50° from a previous value of 60°. By combining both models (double-reflection for incident angles lower than 50° and single-reflection for angles higher), sufficient lighting conditions at 5 m for nearly all incident angles can be achieved. Table 3.1.5 and Figure 3.1.15 show the blind settings and workplane illuminances for this optimal configuration. For incident angles between 35° and 45°, the workplane at a distance of 10 m will receive slightly less than the recommended value of 400 lux. For high solar altitudes, the system is limited by the amount of incident light on the window, which decreases with the cosine of the incident angle.

Table 3.1.5 Workplane illuminance distribution and optimal blind angles for combined single- and double-reflection systems with an 80% spacing (20% blind overlap)

Incident Solar Angle	Even-numbered Blind Angle	Odd-numbered Blind Angle	5-m illuminance [lux]	10-m illuminance [lux]
10°	-41°	-52°	748	447
15°	-37°	-50°	736	440
20°	-50°	-34°	720	430
25°	-30°	-48°	704	421
30°	-27°	-48°	680	406
35°	-24°	-47°	645	386
40°	-20°	-46°	625	374
45°	-16°	-44°	588	352
50°	19°	19°	1,019	671
55°	22°	22°	909	599
60°	24°	24°	792	522
65°	27°	27°	670	441
70°	29°	29°	542	357
75°	30°	30°	345	227
80°	31°	31°	188	124

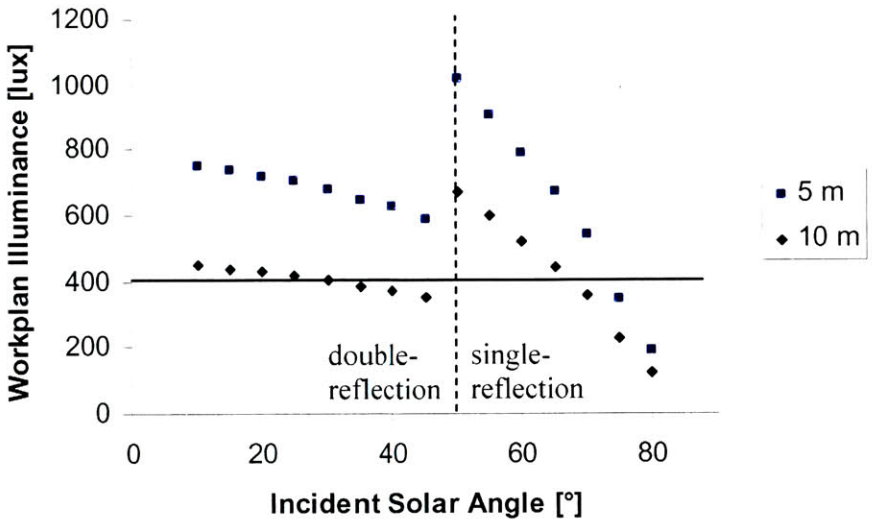

Figure 3.1.16 Workplane illuminance distribution for optimal blind configuration: 80% spacing, combined single and double reflection configurations

Limited access to testing facilities prevented testing of workplane illuminances under direct sun conditions. However, this method can be assumed to be accurate for workplane points in the center of the room (far from walls or other reflective surfaces), as it is a proven method for determining heat transfer between two surfaces. For points at the room perimeter, the effect on workplane illuminance of other surfaces will depend heavily on the reflection coefficients of those surfaces. Additionally, the two-dimensional model assumptions will not predict variances due to changing sun azimuth angle and room geometry in the third dimension.

The current numerical models do not take into account absorption by the glazing material, dirt or dust on the glazing or blind surfaces. The model assumes reasonable but relatively good reflection coefficients for the blind (95%) and ceiling (90%); however, in practice these materials properties may be difficult to achieve. In addition, direct normal illuminance may be less than the assumed 100 klux. As a result, there will be some variability in performance of the system and care must be taken to select blind and ceiling surface coatings with high reflection coefficients.

3.2 Scale Modeling for Direct Solar Incidence

Response to direct solar incidence was simulated using a goniophotometer. This device analyzes the BT(R)DF, or bi-directional (reflection) transmission distribution function, of a given glazing material by measuring the transmitted (or reflected) light in response to an incident collimated beam. Because only the transmitted light (passing directly through the blinds, or reflected inward by the blinds) is of concern for these tests, only the BTDF functionality of the instrument is used.

CIE defines the BTDF of a particular fenestration as the "quotient of the luminance of the medium by the illuminance on the medium." (25) Applied to the case of reflective blinds, the BTDF describes the luminance, as seen from a viewpoint inside the room, as a function of position within the room and incident illuminance on the exterior surface

blinds. The device tests "macro-scale" glazing systems, such as reflective blinds, in addition to smaller scale systems.

Experiments with the goniophotometer are carried out in a 15 x 7 x 8 m dark test chamber designed to minimize reflections. The "walls" are made of heavy black velveteen curtain and the floor is covered in a low-reflectivity black carpet. All surfaces in the chamber are covered with a highly-absorbing material. Thus, parasitic and interior reflected light can be considered negligible. The goniophotometer, shown in the configuration for measurement of BTDF in Figure 3.2.1 and rotated to the BRDF configuration in Figure 3.2.2, directs a collimated light source onto a glazing sample which is mounted on a test bed. The light source simulating the direct component of solar radiation for the goniophotometer at LESO-PB is provided by a stage spotlight. Behind the sample is a diaphragm, smaller in dimension than the sample, which allows light to pass through, after having passed through the sample. This transmitted light then falls on a screen behind the diaphragm, and an image of this screen is then taken by a digital camera. The screen is 1/6 of a cone, and six measurements are taken at six consecutive rotations to make a full cone and to capture the complete light transmission image. The control software is calibrated so that the pixels on the digital images can be translated into luminance data and compared with the direct normal incidence, measured by a photosensor, placed normal to the incident collimated beam. Simulation of different solar positions is achieved by holding the position of the light source constant and rotating the test bed about the three axes.

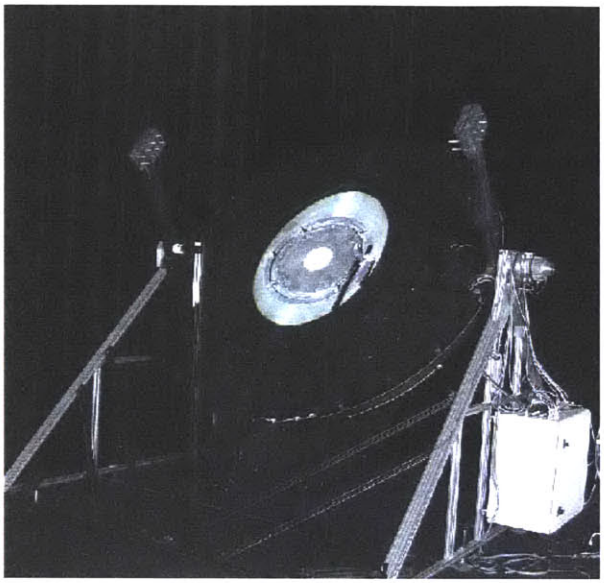

Courtesy: M. Andersen

Figure 3.2.1 Goniophotometer, in transmission configuration

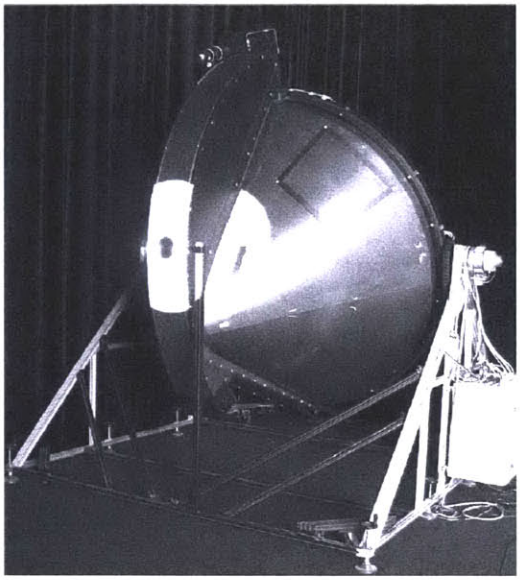

Courtesy: M. Andersen

Figure 3.2.2 Goniophotometer in reflection configuration

The blinds frame is fixed directly to the goniophotometer test bed, as shown in Figure 3.2.3. The smallest diaphragm, 10 cm in diameter, is used in order to achieve the highest angle resolution, 5°. The size of the diaphragm restricts the portion of the blinds participating in the measurement to an area comprising 5 to 6 blind periods. Because the diaphragm is circular, only a small portion of each blind at the top and bottom of the orifice will receive and reflect light. The blinds sample measures 1 cm in thickness, which allows for the desired 1:10 ratio of sample thickness to diaphragm thickness, and this value is used to calibrate the control software. BTDF measurements were conducted for a range of blind configurations and incident solar angles.

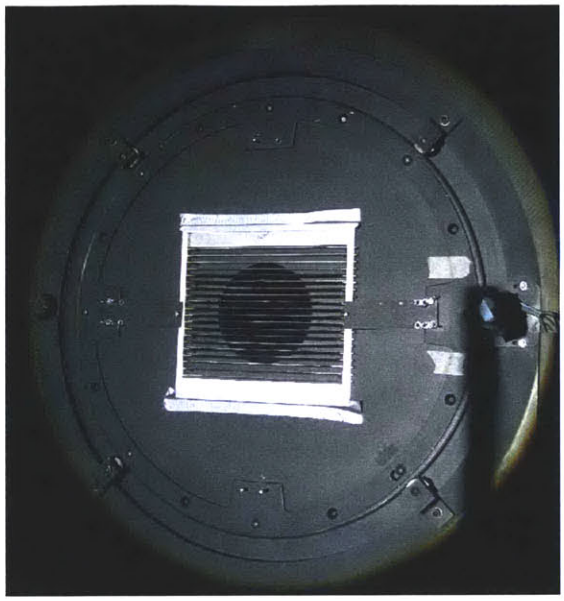

Figure 3.2.3 Blinds frame mounted on goniophotometer in transmission configuration

3.3 Experimental Results

In order to test the validity of the numerical model for direct solar incidence, the goniophotometer was used to measure the BTDF for a range of incident angles and blind configurations.[2] This distribution function is used to determine exit angle from the blinds of the redirected rays, and maximum incident angle without direct penetration, for a given configuration. Table 3.3.1 gives the selected blind angle configurations that were tested and the range of incident solar angles over which each configuration was tested. A blind angle of 0° signifies a horizontal blind position, and this configuration was tested as a reference. A blind with a positive angle is turned in toward the interior, while a negative angle signifies an outward-facing orientation. Configurations requiring shading angles of less than -45° (for incident solar angles of < 43°) were not tested due to limitations of the angle adjustment hardware.

---

[2] Refinements made to the numerical model after the time of experimentation resulted in slight adjustments to the optimal configurations. As a result, values for tested configurations listed in Table 3.3.1 differ slightly from the optimal configurations listed in Table 3.1.2.

Table 3.3.1 Tested blind configurations

Design Incident Solar Angle		45°	55°	60°	70°
Blind Angles	R blinds	16°	22°	24°	29°
	S blinds	-20°	15°	24°	29°

All tests were done using a solar azimuth position of 180° (corresponding to the azimuth position of the sun at solar noon relative to a south-facing façade). As shown in Table 3.3.1, the blinds were set in the optimal configuration for a particular incident solar angle, and this configuration was tested within a range of incident angles above and below this design angle.

The optimal blind angle configuration for a given solar angle blocks all directly transmitted light and redirects light at an angle of approximately 11.3° above the horizontal to reach an approximate target ceiling distance of 10 m in a full-scale room. Tests using incident angles less than the design angle show some directly transmitted rays, while tests using incident angles greater than the design angle should show redirection angles greater than 11.3°. For some of the configurations, results under design conditions show redirected light exiting the blinds at two distinct angles. The rays redirected at the lower angle are reflecting off the *R* blinds. The rays redirected at the higher angle are reflecting off the *S*. In these cases, this light redirected to the front of the room is a residual effect of the blind angle necessary to block directly transmitted rays.

Figure 3.3.1 shows a sample solid three-dimensional BTDF graph. As illustrated, the blinds sample is at the center of the polar axis, the incident rays originate from below and reflected and transmitted rays exit above. As discussed in Section 3.2, the diaphragm exposes 5 to 6 complete blind periods, depending on redirecting and blocking blind angles. As a result, up to 7 blinds may receive and reflect light and the light will emerge from the blinds in up to 7 distinct beams. In most tested configurations, 3 to 4 blinds participate in redirection and 3 to 4 are positioned to block directly transmitted light. The

goniophotometer, however, does not measure the exiting light with a fine enough resolution to capture these distinct beams. In fact, the ratio of the distance between the blinds sample and the image screen to the diameter of the diaphragm is large enough to consider the blinds sample a point source. Therefore, all light exiting the blinds system at a given angle will be measured as a single ray, regardless of the blind from which it originated.

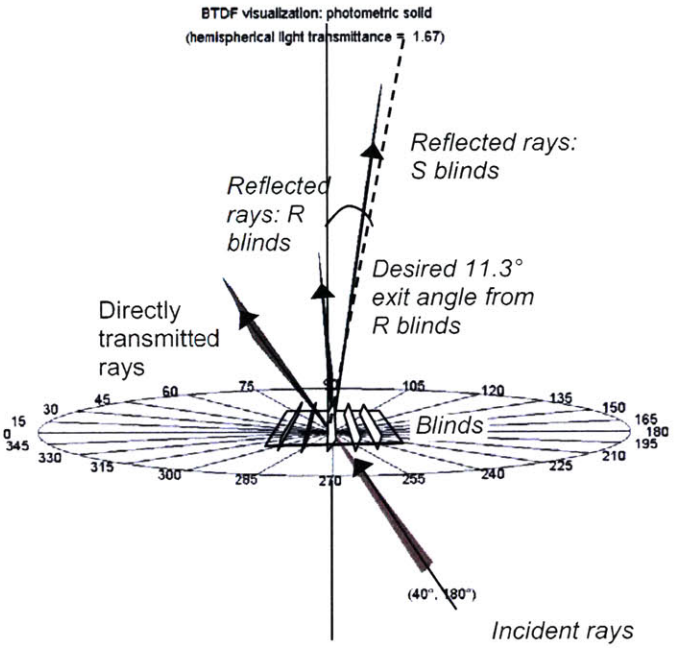

Figure 3.3.1 Sample solid BTDF graph showing blinds and ray orientation

Figure 3.3.2 through Figure 3.3.7 present the response of a configuration optimized for an incident angle of 55° from the horizon. The dotted line represents the target 11.3° exit angle for the rays reflecting off of the redirecting *R* blinds. The redirecting blinds are positioned at 22° while the shading blinds are positioned at 15°. Directly transmitted rays, seen in the first three graphs, exit the blinds at the same angle at which they entered.

Figure 3.3.2 shows the BTDF of the blinds under an incident solar angle of 40°. This incident angle is well below the design solar altitude of 55°, and there is a strong component of directly transmitted light. The two other emergent rays visible in the graph are those redirected by the shading and redirecting blinds. The rays reflected by the redirecting blinds do not exit at the desired angle of 11.3° above the horizontal, but in fact exit at an angle below the horizontal. As the incident angle increases in

Figure 3.3.2 and Figure 3.3.3, the directly transmitted component decreases and the rays reflected by the *R* blinds approach the desired exit angle of 11.3°. At 50°, the directly transmitted component is small, but still present. At 55°, the design incident angle, the directly transmitted component is just blocked and the rays exiting the *R* blinds achieve the desired 11.3° angle as shown in Figure 3.3.5. The angle of the exiting rays from the redirecting *R* blinds at design conditions varied from 11.3° by ± 2°, due to rounding of blind angles and blind angle adjustment error. This variation in blind angle would result in roughly a ± 1 m variation in the position of the light beams on the ceiling.

Appendix C gives the BTDF results for the remaining tested configurations at design conditions. As demonstrated, experimental results confirmed numerical model predictions for shading and redirection and allowed further refinements to the system to be tested using the model with sufficient confidence.

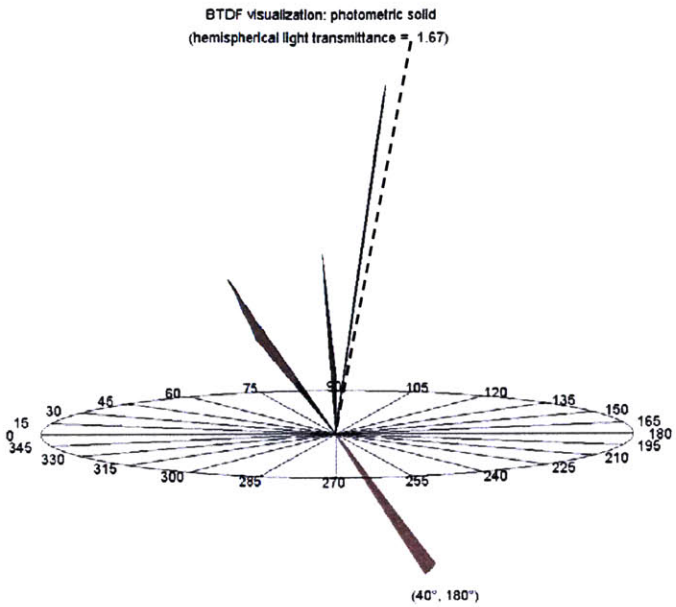

Figure 3.3.2 40° incident solar angle, blinds optimized for 55° incident solar angle

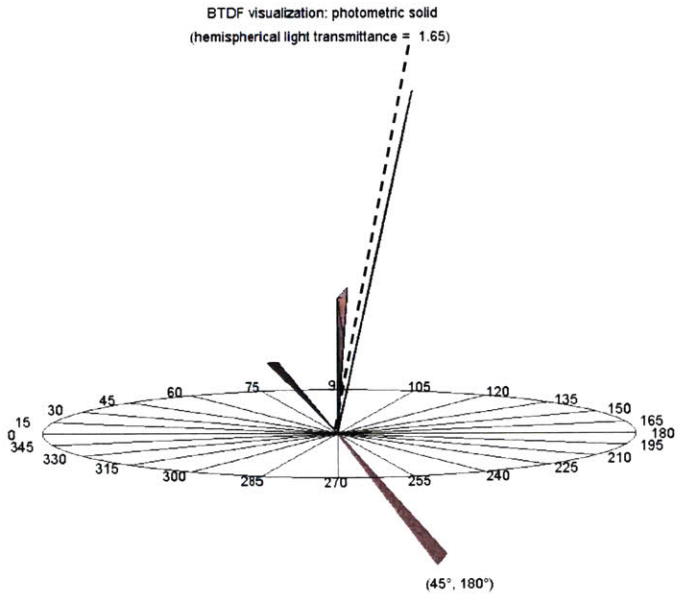

Figure 3.3.3 45° incident solar angle, blinds optimized for 55° incident solar angle

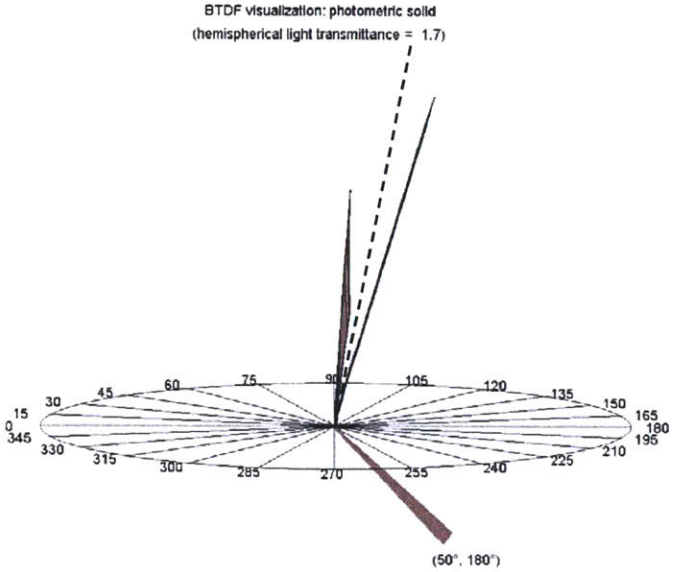

Figure 3.3.4 50° incident solar angle, blinds optimized for 55° incident solar angle

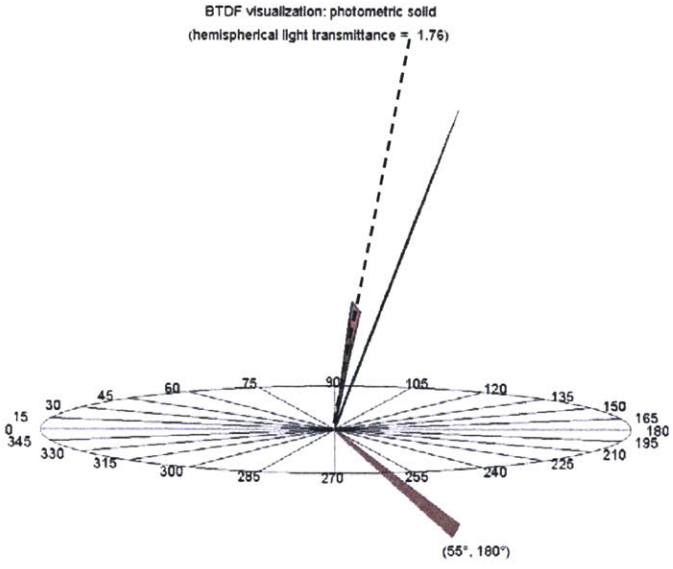

Figure 3.3.5 55° incident solar angle, design conditions

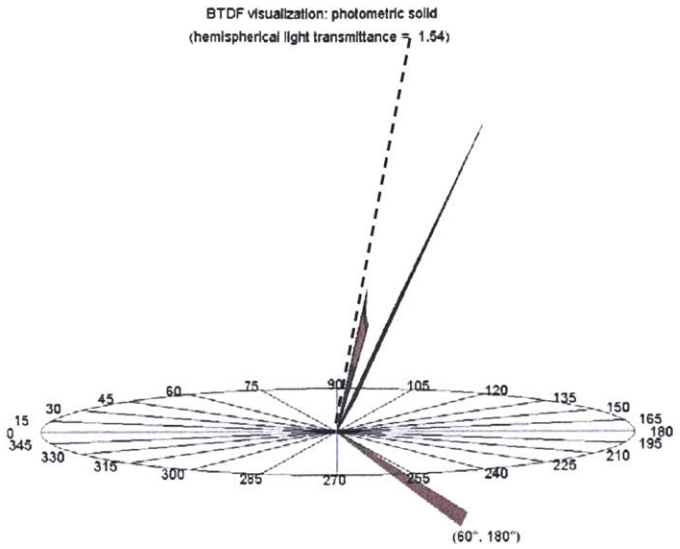

Figure 3.3.6 60° incident solar angle, blinds optimized for 55° incident solar angle

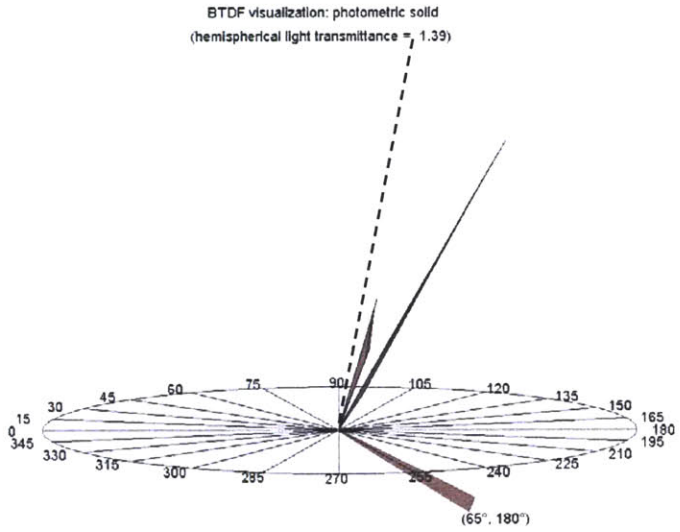

Figure 3.3.7 65° incident solar angle, blinds optimized for 55° incident solar angle

3.4 Integration of Direct Solar and Overcast Models

Direct and overcast numerical models and test simulations indicate that acceptable lighting conditions for distances up to 10 m from the window can be achieved for nearly all sky conditions. A shortened blind spacing is necessary to bring sufficient light deep into the space for direct solar incidence at low incident angles. The overcast model, however, was initially optimized and tested at 100% spacing, and so the implications of this reduced spacing must be examined with the numerical model. Although it is not possible to predict absolute levels of daylight factor at the workplane with the numerical model, the relative impact on light level may be assessed for different blind configurations. This method will be used to predict the change in daylight factor under overcast skies associated with the spacing adjustment that is necessary for the direct solar configurations.

Figure 3.4.1 and Figure 3.4.2 show the previously calculated illuminance ratio distribution for a 100% spacing (blinds are spaced at 100% of blind width) and an optimized blind angle of 21°. Also shown are distributions for two blind configurations at 80% (blinds are spaced at 80% of blind width) spacing, at both the previous specified optimal angle of 21° and the new optimal angle for the 80% configuration, 19°. The optimized configuration for an 80% spacing reduces ceiling illuminance for distances close to the window, up to 3 m. However, at distances greater than 3 m, illuminance ratios are slightly greater than those predicted for the 100% spacing. Although it is not likely this increase of approximately 5% will meaningfully increase workplane daylight factors, it indicates that the reduced spacing will not adversely affect interior light levels.

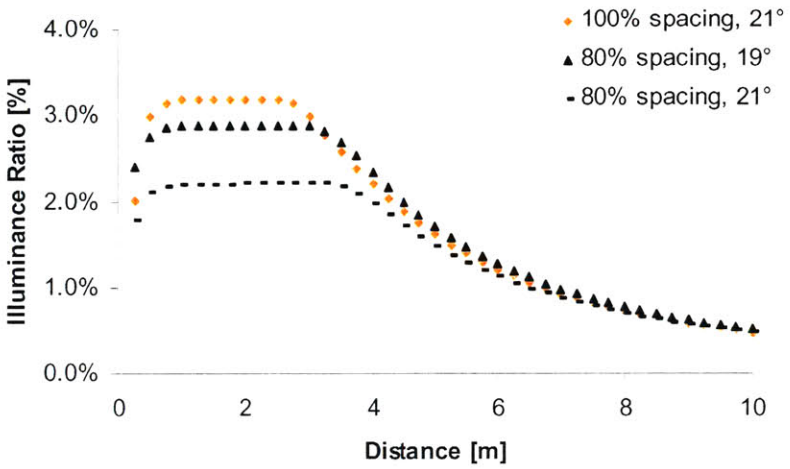

Figure 3.4.1 Model-predicted ceiling illuminance ratio as a function of distance for two spacing configurations under an isotropic overcast sky

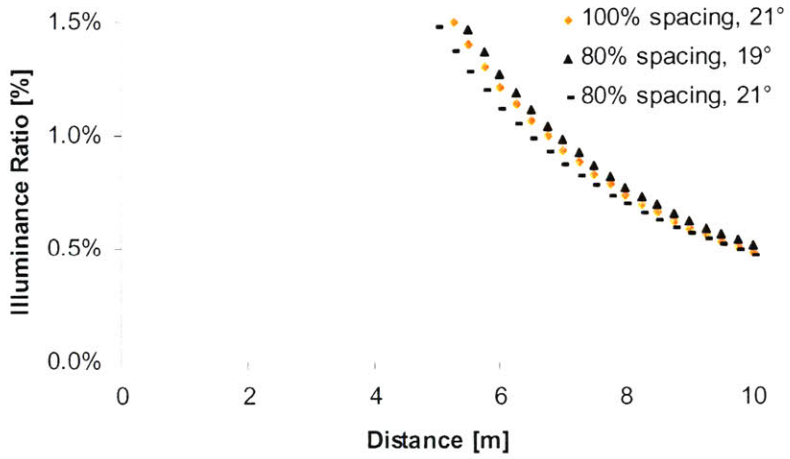

Figure 3.4.2 Model-predicted ceiling illuminance ratio as a function of distance for two spacing configurations under an isotropic overcast sky, shown at an increased scale

4 Conclusion

4.1 Optimal Control Algorithm and Implementation

Making use of the sun's natural light is an effective, attractive, and inexpensive method to light a building. To significantly reduce electric lighting requirements for a building, light should penetrate to a target distance of 10 m from the window. The introduction of natural light into a work space should not cause discomfort for occupants, such as glare or overheating, and should provide sufficient and relatively uniform illumination at work surfaces. Additionally, implementation of such a daylighting solution should be relatively simple and inexpensive.

Properly designed and automated reflective Venetian blinds can achieve comfortable visual conditions through light redirection, allowing nearly a 100% reduction in electric light usage during daylight hours for a 10-meter perimeter from the façade. The blinds provide a fairly even light distribution for both sunny and overcast sky conditions while always providing complete shading from direct solar transmission onto the workplane. Light is redirected by the mirrored blinds to the ceiling, and the highly reflective diffuse ceiling redistributes the light to the workplane below.

This optimal configuration uses alternating shading and light-redirecting blinds under direct sun conditions. Blind angles are finely tuned based on the altitude of the sun, with some blinds performing the shading function while others redirect, and the sun's rays are distributed evenly over a distance of 10 m. For incident sun angles lower than 45° above the horizon, the rays undergo one reflection off the redirecting blinds. For incident angles greater than 45°, the blinds are oriented so that the reflective side of the redirecting blinds is facing upward, and the reflective side of the shading blinds is facing downward. After undergoing two reflections, first off the reflective surface of the upward facing blind and then off the lower reflective surface of the downward facing blind, the rays exit the

blinds, oriented so as to create an equal light distribution. Blind slat spacing is set at an 80% spacing (80% of blind width) to bring in sufficient light at all incident solar angles while still allowing some view to the outside.

Under overcast sky conditions, the amount of available light from the sky is greatly reduced compared with direct sun conditions, but it is still possible to redistribute a meaningful amount of sky light to the rear of the room. This is done by allowing the ceiling at the back of the room to "see" more of the sky through the blinds than it would see simply through an uncovered window. At the 80% blind spacing prescribed by the requirements previously discussed, the blind angle that will allow the ceiling at 10 m to receive the most possible light from the sky is 19°, facing inward toward the ceiling. (At a 100% spacing, the optimal angle changes slightly to 21°).

A combination of numerical computer models and experimental tests were used to confirm these optimal settings. The numerical models made use of the configuration factor method, commonly used in the field of radiant heat transfer. The configuration factor is used to predict the amount of light from one planar source that will be received by another. This method proved to be effective for predicting light contributions from diffuse sources. The two numerical models used in this study have proven reasonably accurate in predicting light level as a function of blind angle, and may be used to test future possible modifications to the system.

Implementation

The successful blind configurations for direct sun redirect a large amount of solar radiation to the ceiling. This causes a temperature rise of the ceiling surface and, by radiant transfer, the air close to the ceiling. In the case of a traditional, well-mixed ventilation system, this might add significant burden on the space's cooling system, tempering the energy savings from turning off the electric lights. Further investigations would quantify the resulting cooling load and balance this against both the energy saved by reducing electric lighting, and the cooling load avoided by not operating the electric lights. Alternatively, this system may successfully complement a buoyancy-driven displacement ventilation system which relies on a larger temperature gradient between workplane and ceiling temperatures.

The final design requires only two independent groupings of blinds, the redirecting blinds and the shading blinds. One possible design for the system uses two motors for independent control of redirecting and shading blinds. The reflective slats might be encased between two pieces of glazing in an integrated blinds system, in order to reduce dirt and dust accumulation on the highly reflective surfaces. A dual-motor system would not likely provide significant design challenges to implementation (as, say, a 20-motor system would). Currently manufactured dual-motor blind systems might be modified to control alternating blinds without significant redesign.

4.2 Future Work

Solar Azimuth Angle

The final blind operation sequence is optimized to handle all incident solar altitudes, but does not take into account azimuth angle. If the blinds are implemented along a façade that is relatively long compared to room depth, then variances due to changing solar azimuth will affect only the back corners of the space and the blinds will still function to light a large portion of the space. If, however, the façade length is roughly the same as the room depth, then there will be a significant portion of the room that is not lit when the solar rays are at wide azimuth angles relative to the window. Figure 4.2.1 shows two simplified floor plans; one exhibits a 1:1 length to depth ratio and the other a 3:1 ratio. As demonstrated, the plan with a larger length to depth ratio still receives reflected light to a large portion of the floor plan at an azimuth angle of 45°. However, the plan with a 1:1 ratio loses lighting to half the space at a 45° incident angle.

In this case, it may be preferable to install a second layer of blinds, oriented vertically, outside the horizontal blinds. These blinds would adjust relative to the sun's azimuth angle so that all rays entering the horizontal blinds would do so from the normal direction to the window, as shown in Figure 4.2.2. This second set of blinds, however, would further reduce the view to the outside, and so an alternative design would be preferable. For floor plan spaces that border more than one façade, it may be possible to place blinds on the additional facades to reduce the losses due to azimuth angle changes, also shown in Figure 4.2.2.

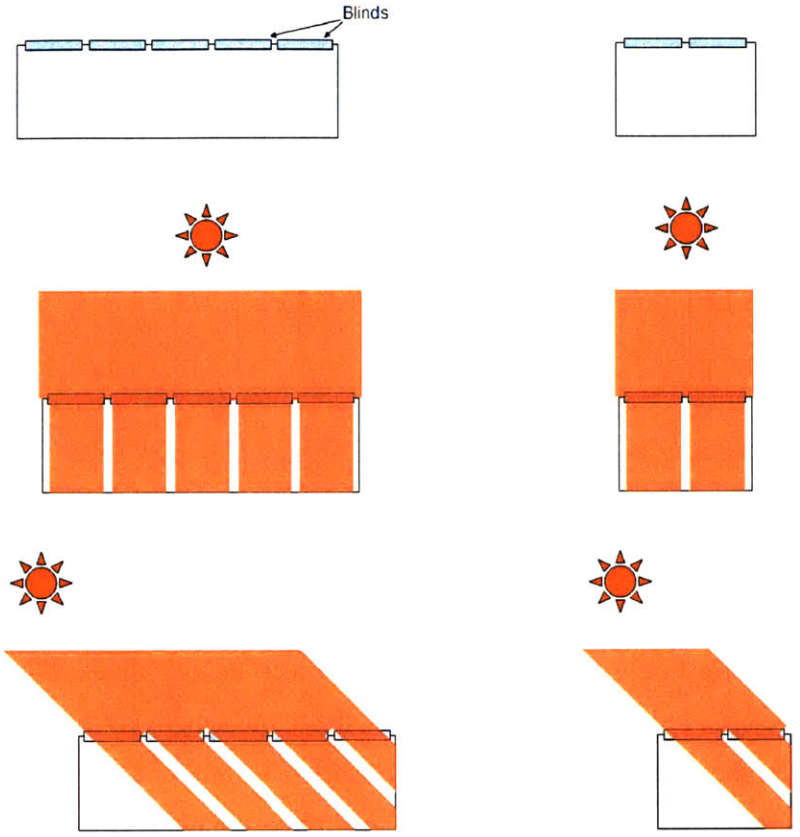

Figure 4.2.1 Light redirection patterns for two floor plan sizes, for azimuth angles of 0° and 45° from normal

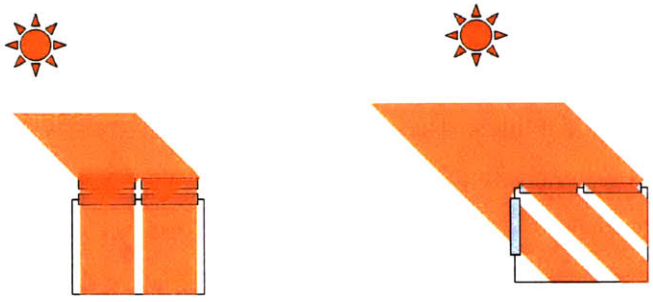

Figure 4.2.2 Possible alternatives for small floor plan to increase percent of floor plan that receives light

Experimental Confirmation

Workplane illuminance due to ceiling illumination from direct sun was modeled using configuration factors, and favorable illumination was achieved at nearly all workplane locations. However, additional testing of the performance of this system would be preferable to verify these predicted values. These tests would require an additional test apparatus (neither the heliodon/sky simulator nor the goniophotometer can measure interior workplane illuminances under these conditions) or perhaps full-scale simulation.

Additionally, only two sky conditions were modeled and tested. A full-scale mock-up tested under real-sky conditions would yield performance data for intermediate sky types.

Blind Slat Modifications

The blinds were modeled and tested with diffuse black lower surfaces. Adding a diffuse white coating to the lower surface of each blind may increase light penetration, especially under overcast skies. This scenario would be difficult to replicate in the existing numerical models, and might be better examined either in RADIANCE or in an experimental setting.

Additionally, further work should be done to analyze the impact of blind geometry on light distribution. Typically, in order for a standard Venetian blind to be made rigid, the blind is given a slight curvature during the manufacturing process. The numerical models developed for the design described herein use virtual sky images constructed using reflections on flat surfaces. This modeling technique would no longer hold for more complex geometries. For curved blinds, a ray tracing software could be used.

Thermal Performance

In order to minimize energy consumption of the building system (not just of lighting energy), it is necessary to model the thermal performance of the lighting system. The redirection of direct solar radiation will add significant cooling loads to the building's HVAC system. It is recommended that this heat addition be measured against the energy savings gained from reducing electric light consumption (and the accompanying heat generated by the lights), in order to determine the optimal control system to minimize overall building energy consumption, while meeting the comfort needs of occupants.

Appendices

Appendix A

Percentage contribution of each blind to total ceiling illuminance at 10 m based on a 30 klux sky plane exitance

Blind	Angle [°]	Contribution [lux] (% of total, 154 lux)	Angle [°]	Contribution [lux] (% of total, 151 lux)	Angle [°]	Contribution [lux] (% of total, 146 lux)
1 (top)	26	1 (0.4%)	24	1 (0.4%)	21	1 (0.4%)
2	25	1 (0.9%)	24	1 (0.9%)	21	1 (0.8%)
3	25	2 (1.3%)	24	2 (1.3%)	21	2 (1.2%)
4	25	3 (1.8%)	24	3 (1.8%)	21	2 (1.7%)
5	24	4 (2.3%)	24	3 (2.3%)	21	3 (2.1%)
6	24	4 (2.7%)	23	4 (2.7%)	21	4 (2.6%)
7	24	5 (3.2%)	23	5 (3.2%)	21	5 (3.1%)
8	23	6 (3.7%)	23	6 (3.7%)	21	5 (3.6%)
9	23	6 (4.2%)	23	6 (4.3%)	21	6 (4.2%)
10	23	7 (4.7%)	23	7 (4.7%)	21	7 (4.7%)
11	22	8 (5.2%)	21	8 (5.1%)	21	8 (5.3%)
12	22	9 (5.7%)	21	9 (5.6%)	21	9 (5.9%)
13	22	10 (6.2%)	21	9 (6.2%)	21	9 (6.4%)
14	21	10 (6.7%)	21	10 (6.8%)	21	10 (7%)
15	21	11 (7.2%)	21	11 (7.3%)	21	11 (7.6%)
16	21	12 (7.7%)	20	12 (7.7%)	21	12 (8%)
17	20	13 (8.2%)	20	13 (8.3%)	21	12 (8.3%)
18	20	13 (8.7%)	20	13 (8.9%)	21	13 (8.7%)
19	20	14 (9.3%)	20	14 (9.2%)	21	13 (9%)
20 (bottom)	19	15 (9.8%)	20	14 (9.5%)	21	14 (9.3%)

Appendix B

Predicted workplane illuminance distributions for various incident angles for three blind configurations in response to an incident illuminance of 100 klux, measured in the normal direction of the incident rays

Double-reflection scenario, blind spacing 100%

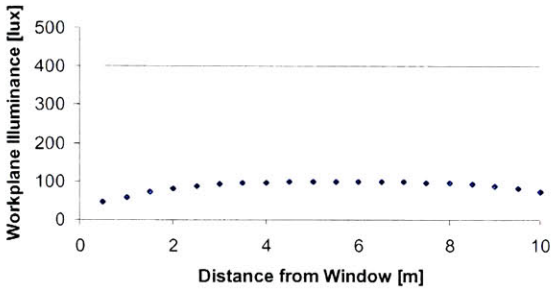

10° incident solar angle

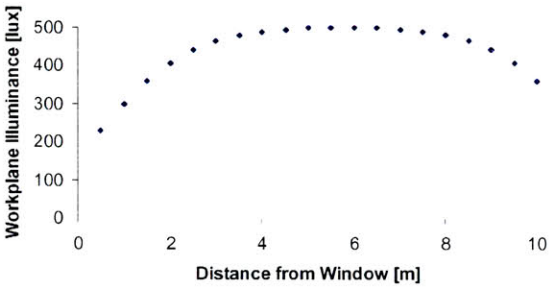

25° incident solar angle

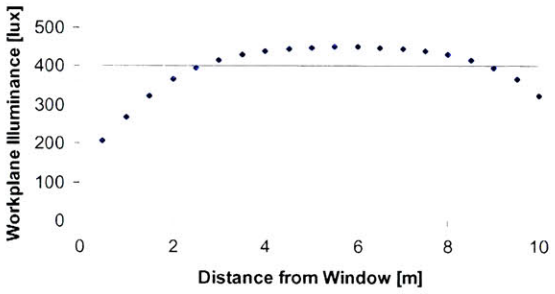

45° incident solar angle

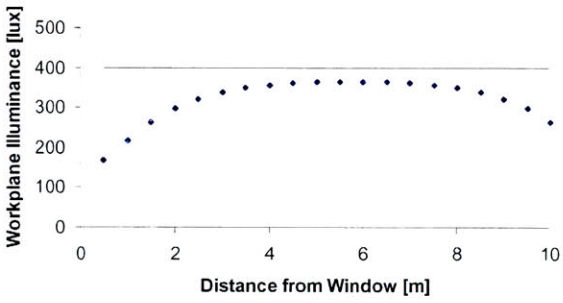

60° incident solar angle

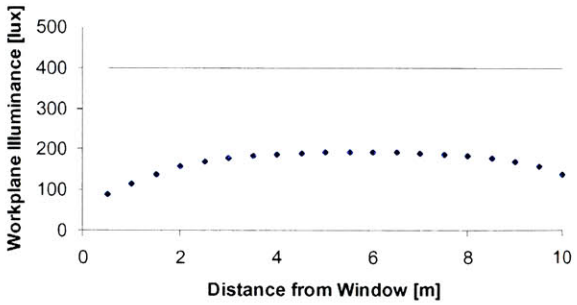

75° incident solar angle

Double-reflection scenario, blind spacing 80%

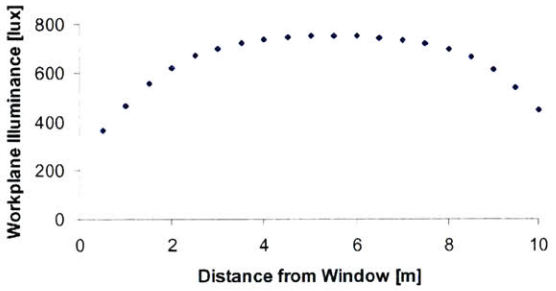

10° incident solar angle

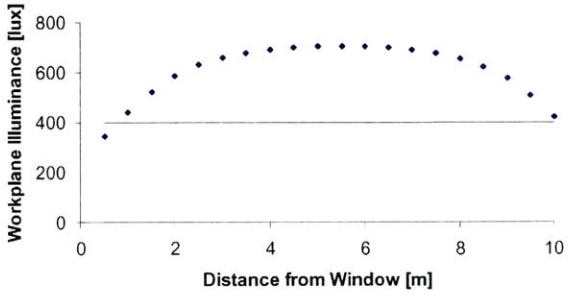

25° incident solar angle

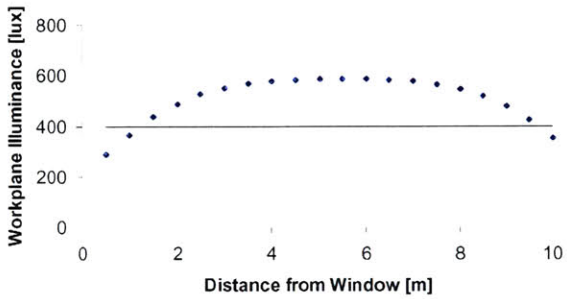

45° incident solar angle

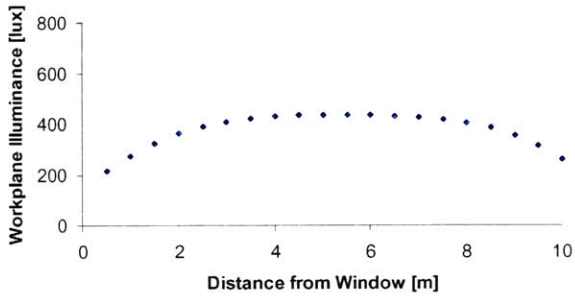

60° incident solar angle

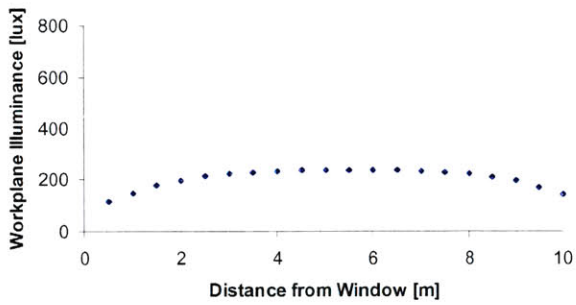

75° incident solar angle

Single-reflection scenario, all blinds participate in redirection, blind spacing 80%

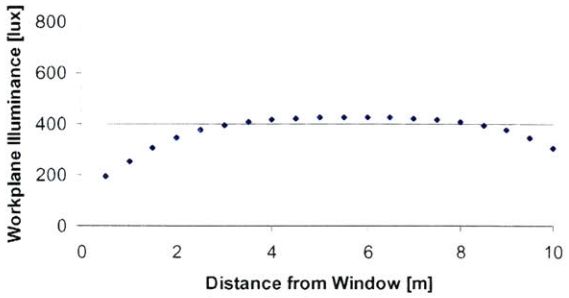

45° incident solar angle

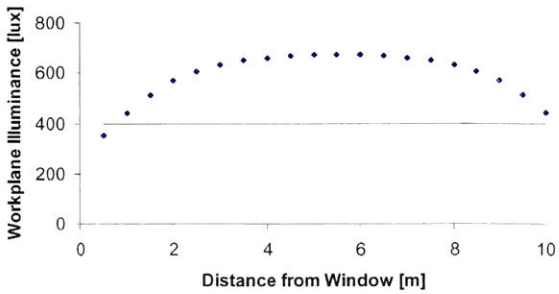

60° incident solar angle

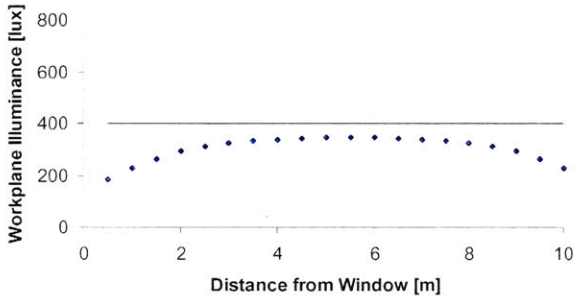

75° incident solar angle

Appendix C

BTDF results for three blind configurations, optimized for incident solar angles of 45°, 60°, and 70°

BTDF at varying incident solar angles for a configuration design angle of 45°

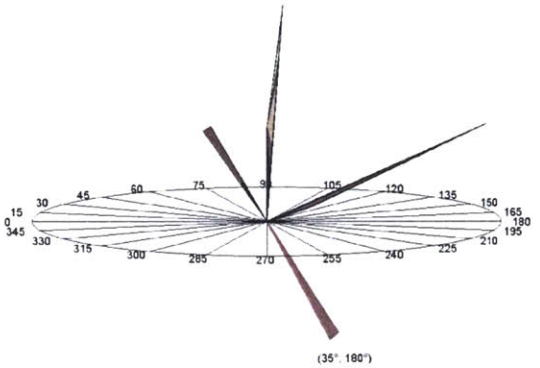

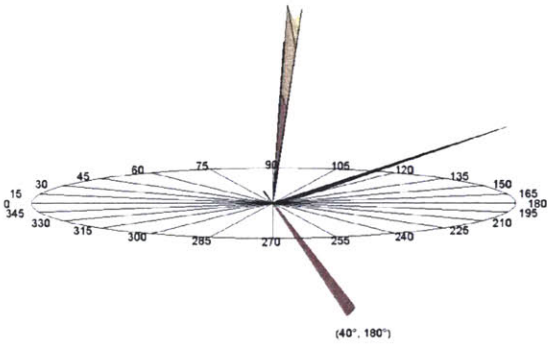

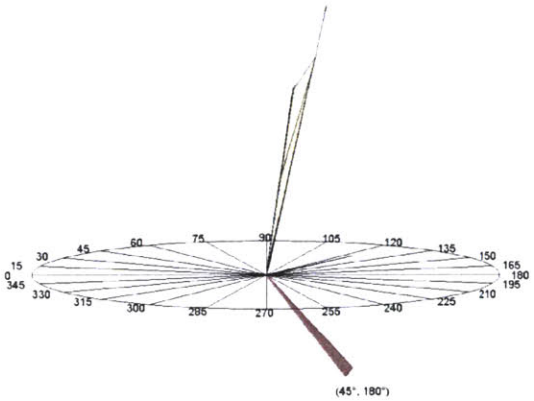

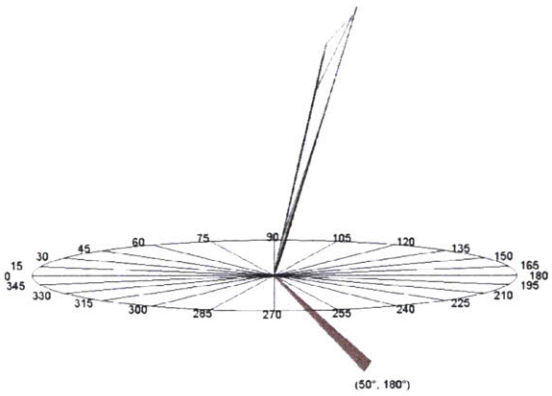

BTDF at varying incident solar angles for a configuration design angle of 60°

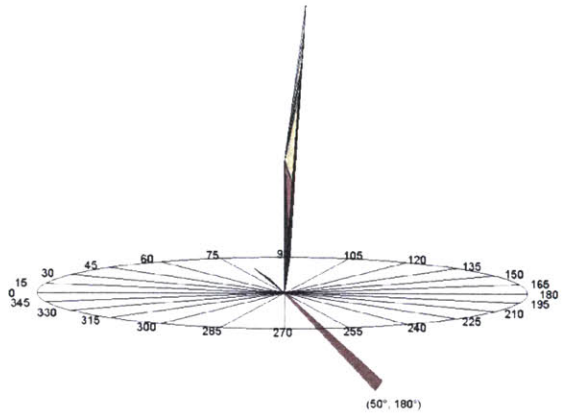

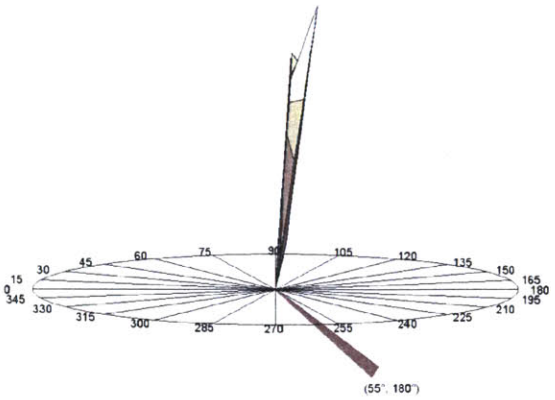

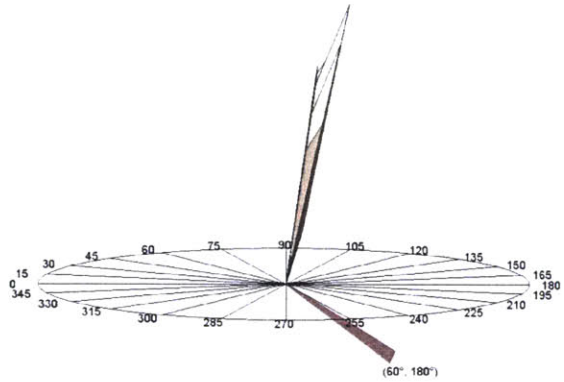

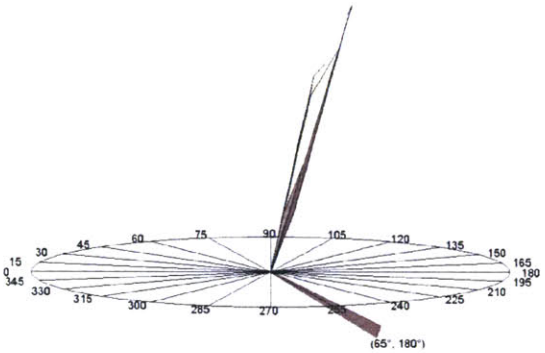

BTDF at varying incident solar angles for a configuration design angle of 70°

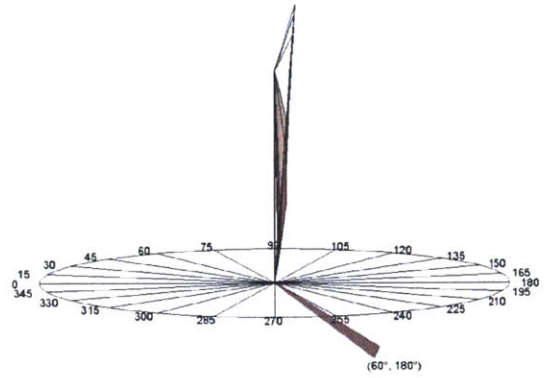

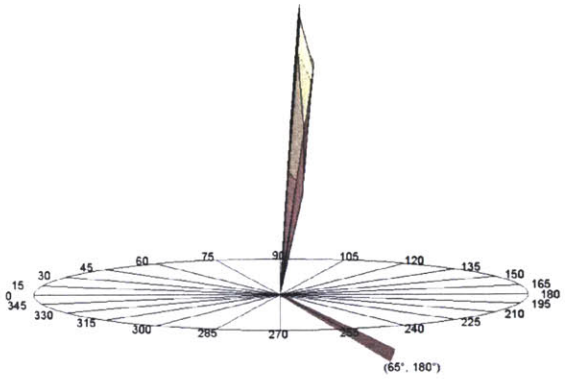

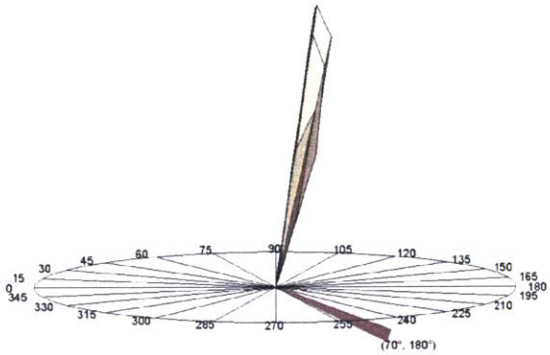

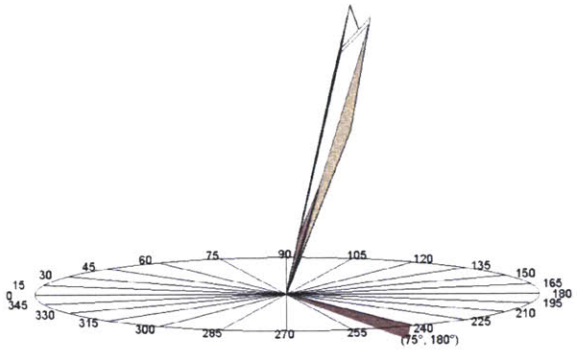

Appendix D

Nomenclature

Photometric quantities

Q	Flux [lm]
L	Luminance, or flux in a given direction by a given surface $\left[\frac{lm}{sr \cdot m^2}\right]$ or $\left[\frac{cd}{m^2}\right]$
E	Illuminance, or flux received by a given surface $\left[\frac{lm}{m^2}\right]$ or $[lux]$
$F_{A\text{-}B}$	Configuration factor between planar surfaces A and B
M	Exitance, or flux emitted by a given surface $\left[\frac{lm}{m^2}\right]$ or $[lux]$
BTDF	Bi-directional Transmission Distribution Function $\left[\frac{cd}{m^2 \cdot lux}\right]$ or $\left[\frac{1}{sr}\right]$

Other

B	Incident solar angle [°]
θ	Blind angle [°]
α	Exit angle of ray from blind [°]

References

(1) Solar Energy International. *Energy Facts.* http://www.solarenergy.org/ resources/ energyfacts.html (2005).

(2) U.S. Department of Energy, Energy Information Administration. *Monthly Energy Review.* April (2005)

(3) Ander, G. *Daylighting Performance and Design.* 2nd Ed, John Wiley & Sons, NJ (2003).

(4) Heschong, L., Heschong Mahone Group, *Daylighting in Schools, An Investigation into the Relationship Between Daylighting and Human Performance, A report to Pacific Gas and Electric Company.* CA (1999).

(5) New Building Institute, Re-Analysis Summary, Daylighting in Schools, Additional Analysis, A Report to the California Energy Commission, Public Interest Research Program (PIER) (2001).

(6) Romm, J., W. Browning. *Greening the Building and the Bottom Line: Increasing Productivity through Energy Efficient Design.* Rocky Mountain Institute, CO (1994).

(7) Beltràn, L.O., E.S. Lee, S.E. Selkowitz, "Advanced Optical Daylighting Systems: Light Shelves and Light Pipes," Procedings of the 1996 IESNA Annual Conference, August 4-7, Cleveland, OH (1996).

(8) Behnisch, Behnisch & Partner, Artchitects, text by James Steele. *Genzyme Center.* FMO Publishers (2004).

(9) International Energy Agency (IEA) Solar Heating and Cooling Programme, Energy Conservation in Buildings & Community Systems, *Daylighting in Buildings: A Source Book on Daylighting Systems and Components (a report of IEA SHC Task 21/ECBCS Annex 29).* Berkeley, CA (2000).

(10) Walker, C., L. Glicksman, L. Norford, *Assessing the Performance of a Naturally Ventilated Office Building: Houghton Hall, Luton, UK* ASHRAE Syposium Paper (under review). Low Energy Buildings Through Integrated Design, January (2006).

(11) Beltran, L.O., E.S. Lee, K.M. Papamichael, S.E. Selkowitz, "The Design and Evaluation of Three Advanced Daylighting Systems: Light Shelves, Light Pipes, and Skylights," Solar '94 Conference Proceedings, June 25-30, San Jose, CA (1994).

(12) Lee, E.S., D.L. DiBartolomeo, S.E. Selkowitz. "Thermal and Daylighting Perfomance of an Automated Venetian Blind and Lighting System in a Full-scale Private Office." *Energy and Buildings* 29, 47-63 (1998).

(13) Rosenfeld, A.H., S.E. Selkowitz, "Beam Daylighting: an Alternative Illumination Technique." *Energy and Buildings* 1, 43-50 (1977).

(14) Breitenbach, J., S. Lart, I. Langle, J.L.J. Rosenfeld. "Optical and Thermal Performance of Glazing with Integral Venetian Blinds." *Energy and Buildings* 33, 433-442 (2001).

(15) Tzempelikos, A., A.K. Athenitis. "Modeling and evaluation of a window with integrated motorized venetian blinds." ISES Solar World Congress 2003 Procedings, Solar Energy for a Sustainable Future, Göteborg, Sweden, June 14 – 19 (2003).

(16) Illuminating Engineering Society of North America (IESNA) (Ed: Rea, M.), *Lighting Handbook 9th Edition*. New York, NY (2000).

(17) Thanachareonkit, A., J.-L. Scartezzini, M. Andersen. "Comparing daylight performance assessment of buildings in scale models and test modules." Solar Energy, Article in press, January (2005).

(18) Veitch, J.A., Newsham, G.R. "Preferred luminous conditions in open-plan offices: Research and practice recommendations." Lighting Research and Technology, 32(4), 199-212 (2000).

(19) CIE. Lighting of Indoor Work Places (Joint ISO/CIE Standard), ISO 8995:2002/CIE S 008/E (2001).

(20) US. Dept of Energy, Energy Efficiency and Renewable Energy, Building Technologies Program website. *Building Toolbox: Daylighting.* url: http://www.eere.energy.gov/buildings/info/design/integratedbuilding/passivedaylighting.html#daylight (2005).

(21) Hottel, H. C.: "Radiant Heat Transmission," in *Heat Transmission*, ed. W. H. McAdams, 3d ed., ch. 4, McGraw-Hill, NY (1954).

(22) Andersen, M.. *Innovative bi-directional video-goniophotometer for advanced fenestration systems*. PhD thesis, EPFL, Lausanne (2004).

(23) Michel, L., C. Roecker, J.-L. Scartezinni. "Performance of a new scanning sky simulator." Lighting Research and Technology 27(4), 197 – 207 (1995).

(24) Mardaljevic, J. "Quantification of parallax errors in sky simulator domes for clear sky conditions. Lighting Research and Technology," 34(4), 313-332 (2002).

(25) Commission Internationale de l'Eclairage. Radiometric and photometric characteristics of materials and their measurements. CIE, 38(TC-2.3) (1977).